# Chapter 13*

# STABILITY ANALYSIS OF SLOPES AND PROBABILITY OF SLOPE FAILURE

## 13.1 PURPOSE OF SLOPE STABILITY ANALYSIS

Slope stability analysis is the most important aspect relating to any infrastructure in the mountain areas. Engineering a structure in the hilly or mountainous areas involves analysis of slopes, both failed and unfailed, so that the level of risk and the associated mitigatory measures can be decided. Recently major landslides in the *Himalaya* have started causing panic to the public. Hence the importance of the subject.

A thorough slope stability analysis is a complex and involved task requiring theoretical understanding and experienced judgement relating to geological processes, soil and rock mechanics, and practicable remedial measures. The level of rigor that needs to be applied to the slope in question depends upon the size and nature of the problem. Understanding of the basic principles and techniques of the stability analysis of soil and rock slopes is a must for every one or, at least, for the engineer who wishes to work by taking natural processes into account.

The following are the main purposes of slope stability analysis.

- To assess potential hazard associated with natural slopes.
- To determine stable slope angles for proposed cut slopes.
- To decide appropriate remedial measures for improvement of the stability of cut slopes or existing landslides.

A package of computer programmes makes analysis and design interesting and time-saving, but it pays to understand the mechanisms of landslides.

## 13.2 LEVELS OF SLOPE STABILITY ANALYSIS

Projects such as roads and canals cover a large area. The stability assessment for various stages of a project cycle should be different.

### 13.2.1 *Network Level Planning*

Screening of several alternatives for the purpose of investment planning needs rapid methods of stability assessment. Different instability criteria are grouped, weighted, and rated for different sections of the various alternatives.

---

* Figures and Tables without credit lines in this Chapter are compiled by the author.

### 13.2.2 *Project Level Planning*

Once the alternatives are compared and reduced to one or two, detailed hazard mapping is necessary to develop tentative designs and cost estimates after matching the specified project to the natural processes. Hazard maps and their supporting maps provide a complete picture of geological structures, material types, geo-dynamical processes, and terrain slopes. Identification of areas requiring various levels of rigor for slope stability analysis is possible from these maps.

### 13.2.3 *Implementation Level*

The implementation level here implies the stages wherein detailed design and subsequent construction are carried out. Stability assessment during detailed design involves:

- minimal investigations and quick methods to determine stable slope angles in low height cuts and in low hazard areas. Chart solutions are generally adequate for such areas;
- intensive investigations and standard solutions to determine stable cut slope angles and minor remedial measures for areas involving medium height of cuts and medium hazard levels; and
- rigorous investigations and analysis to determine stable cut slope angles and major remedial measures for areas in high cuts and in high hazard levels.

Stability assessment during the construction stage is just a repetition of the above steps for differing site conditions.

## 13.3 STABILITY ANALYSIS OF SOIL SLOPES

In mountain areas, it is rarely possible to find slopes with soils of an infinite depth. Solid or jointed bedrocks are mostly encountered within a few metres of residual or colluvial soils. Colluvial soil, in excess of 30 metres in depth, is also encountered in some hill areas of the *Lesser Himalaya*.

For the purpose of slope stability analysis, all slopes whose stability is governed by failure of the soil mass overlying the rockbed should be treated with soil slope stability analysis.

Slopes, irrespective of the thickness of overlying soil, that are failing primarily from the failure of underlying rocks should be dealt with under rock slope stability.

Two basic approaches to soil slope stability analysis with respect to mode of failure are 1) limit equilibrium analysis and 2) deformation analysis. Most of the methods so far available fall into the former category.

The limit equilibrium method of analysis is based on an assumed failure plane and the assumption that Coulomb's Failure Criterion is satisfied along the failure surface. Stress-strain relationship and *in situ* stresses are not considered and the deformation cannot be predicted by this method. The two-dimensional computer methods of analysis described in this chapter are limited to this method only in view of the

simplicity and adequacy for most infrastructural problems of infrastructures in developing countries. The shear strength parameters such as cohesion (c) and angle of friction ($\phi$) used in most soil slope analyses are based on either total stress or effective stress. It is essential to understand the relevance of these parameters to design requirements.

### 13.3.1 *Total Stress and Effective Stress*

The shear strength parameters, such as c and $\phi$, to be used in the stability analysis are obtained from laboratory tests or *in situ* direct shear test or back analysis of failed slope or standard tables. These parameters must represent the actual field conditions which have soil mass in either drained or undrained conditions.

When a saturated soil is sheared to failure without permitting drainage, the soil behaves as though it is purely cohesive, i.e., $\phi = 0$ and the shearing strength is the shear strength from undrained shear test in the laboratory. This condition may be representative of field conditions where pore pressures are governed by total stress changes and little time has elapsed so that no significant dissipation has occurred. This is also called an end-of-construction class of problem, e.g., stability of road embankments just after construction or landslide by liquefaction.

The usual conditions for most natural slopes of soil and rock are governed by steady seepage configurations, and stability analysis for such cases should be performed in terms of effective stresses. This is a case of long-term conditions which applies to most permanent cuts and fills and road embankments.

In total stress analysis it is implied that the pore-water pressures are those for failure conditions. In effective stress analysis, the pore-water pressures used are those predicted for existing (non-failure) conditions.

An effective stress analysis is relevant for all conditions where values of pore-water pressure are obtained from the static water table level or the appropriate flow net. Pore-water pressure may thus be an independent variable, determined from the static water table or from the flow net for steady seepage conditions. There is some misconception that seepage lubricates soil and rock and causes landslides. Actually effective stress (and not friction) is reduced.

The method adopted for the slope stability analysis of practical problems should be based on identification of the most dangerous conditions during the service life of the designed slope. Shear strength parameters for use in design are those representing the most dangerous conditions. Experience and judgements are necessary to predict probable changes in conditions between site investigation and the worst time during the design life of the slope.

### 13.3.2 *Analysis of Infinite Slope and Plane Translational Failures* (Fig. 13.1)

This is a very common mode of failure of talus along roads.

A) *Factor of Safety*

Consider a prism, in Figure 13.1 of inclined length 1 x sec ß, unit width and height H:

Factor of safety,

$$F.S. = \frac{Shearing\ Resistance}{Shearing\ Force} = \frac{\tau}{T}$$

Shearing Force,

$$T = (W + q_o) \sin\beta$$

Weight,

$$W = [\gamma\ (H-H_w) + \gamma sat \times H_w]$$

$$\therefore\ T = \sin\beta\ [(q_o + \gamma H) + H_w\ (\gamma sat - \gamma)]$$

Shearing resistance using Coloumb's equation,

$$\tau = (c' + \sigma' \tan\phi') \sec\beta + q_o \cos\beta \tan\phi'$$

$$= \frac{[(c' + \sigma' \tan\phi') + q_o \cos^2\beta \tan\phi']}{\cos\beta}$$

$$= \frac{[c' + (\sigma - u) \tan\phi' + q_o \cos^2\beta \tan\phi']}{\cos\beta}$$

Normal Stress,

$$\sigma = \gamma(H-H_w) \cos^2\beta + \gamma sat \times H_w \cos^2\beta$$

$$= \cos^2\beta\ [\gamma H - \gamma H_w + \gamma sat\ H_w]$$

$$= \cos^2\beta\ [\gamma H + H_w\ (\gamma sat - \gamma)]$$

Pore Pressure,

$$u = \gamma_w H_w \cos^2\beta$$

$\gamma_w$ = *unit weight of pore fluid*

Effective Stress,

$$\sigma' = \sigma - u = \cos^2\beta\ [\gamma H + H_w\ (\gamma sat - \gamma_w - \gamma)]$$

$$\therefore\ \tau = \frac{[c' + \tan\phi'\ \cos^2\beta\ \{q_o + \gamma H + H_w\ (\gamma sat - \gamma_w - \gamma)\}]}{\cos\beta}$$

$$= \tan\phi'\ \cos\beta\ [\frac{c'}{\cos^2\beta\ \tan\phi'} + (q_o + \gamma H) + H_w\ (\gamma sat - \gamma_w - \gamma)]$$

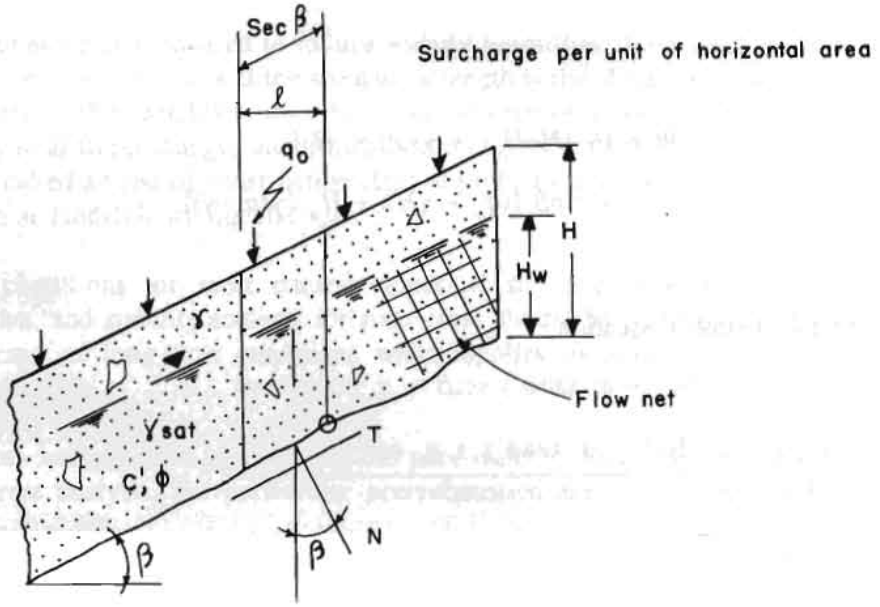


Source: Gray and Leiser 1982

**Fig. 13.1 Idealized infinite slope**

Factor of safety,

$$F.\ S. = \frac{\tan\phi'\ \cos\beta\ [\frac{c'}{\cos^2\beta\ \tan\phi'} + (q_o + \gamma H) + H_w\ (\gamma sat - \gamma_w - \gamma)]}{\sin\beta\ [(q_o + \gamma H) + H_w\ (\gamma sat - \gamma)]}$$

$$F.\ S. = \frac{\frac{\tan\phi'}{\tan\beta}\ [\frac{c'}{\cos^2\beta\ \tan\phi'} + (q_o + \gamma H) + H_w\ (\gamma sat - \gamma_w - \gamma)]}{[(q_o + \gamma H) + H_w\ (\gamma sat - \gamma)]} \qquad (13.1)$$

The above equation may be generalised easily for seismic conditions (Ranjan et al. 1984). It may be noted that surcharge $K$ (e.g., trees) increases the factor of safety if $C < \gamma_w H_w \tan\phi \cos^2\beta$. One may further note that $H$ represents the average depth of the debris on rock in case of a slightly non-uniform slope surface.

For cohesionless soil with surcharge and water level at ground surface:

$$F.S. = \frac{\tan\phi'}{\tan\beta} \left[\frac{(q_o + \gamma H) + H_w (\gamma sat - \gamma_w - \gamma)}{(q_o + \gamma H) + H_w (\gamma sat - \gamma)}\right] .$$

For cohesionless soil and water level at ground surface but no surcharge:

$$F.S. = \frac{\tan\phi'}{\tan\beta} \left[\frac{(\gamma sat - \gamma_w)}{\gamma sat}\right] \qquad (13.2)$$

and in seismic cases (Ranjan et al. 1984)

$$F.S. \approx \frac{\tan\phi}{\tan(\beta + \lambda)} \left[\frac{\gamma sat - \gamma_w}{\gamma sat}\right] \quad ;$$

$\tan\lambda$ = horizontal component of earthquake acceleration.

For cohesionless dry soil and no surcharge

$$F.S. = \frac{\tan\phi'}{\tan(\beta+\lambda)} .$$

Thus, it may be noticed that saturated slopes in cohesionless soil, having a saturated unit weight of 2.0g/cc result in a factor of safety which is half of that for a cohesionless dry soil. This is the cause of talus failures/debris slides in rainy season due to temporary rise in the perched water table. (It may be noted that the drag force on boulders, caused by high seepage velocity, has been neglected in Eq. 13.2.)

It may also be noted that a dry slope underlain by sand is stable, regardless of the height and surcharge, provided the angle ß between the slope and horizontal is equal to or less than the angle of internal friction $\phi$ for the sand in a loose state (and $\phi - \lambda$ in seismic cases).

The computer programme Stability Analysis of Slope with Talus Deposit (SAST) may be used to compute factors of safety with and without earthquake forces. It also gives remedial measures. The programme Back Analysis of Slope with Talus Deposit (BAST) performs analysis of failed talus slopes.

B) *Stability Number for Soil with Cohesion and Friction: Case of Infinite Slope*

Rewriting equation (13.1) for a factor of safety of 1.0, and for water table at surface and no surcharge:

$$c' + [(q_o+\gamma H) + H_w\ (\gamma sat-\gamma_w-\gamma)]\ \tan\phi'\ \cos^2\beta = \cos\beta\ \sin\beta\ [(q_o+\gamma H) + H_w\ (\gamma sat-\gamma)]$$

or,

$$c' = H\ \gamma sat\ \sin\beta\ \cos\beta - H(\gamma sat - \gamma_w)\ \tan\phi'\ \cos^2\beta$$

$$= H\ [\gamma sat\ \sin\beta\ \cos\beta - \gamma_b\ \tan\phi'\ \cos^2\beta]$$

$$\gamma_b = \textit{buoyant unit weight}$$

$$= H\ \gamma sat\ \cos^2\beta\ (\tan\beta - \frac{\gamma_b}{\gamma sat}\ \tan\phi')$$

or,

$$\frac{c'}{H\ \gamma sat} = \cos^2\beta\ (\tan\beta - \frac{\gamma_b}{\gamma sat}\ \tan\phi') \quad .$$

Substituting $1/N_s$ (stability number) for right hand side of the eqn., we get:

$$\frac{c'}{H\ \gamma sat} = \frac{1}{N_s} \quad .$$

Treating this height when the factor of safety becomes 1.0 as the critical $H_c$,

$$\frac{c'}{H_c\ \gamma sat} = \frac{1}{N_s}$$

$$\therefore\ H_c = N_s\ \frac{c'}{\gamma sat} \quad .$$

13.3.3 *Debris Flow*

Figure 13.2. illustrates the mechanism of debris flows along gullies. First of all, rainstorm causes landslides on the top, steep parts of gullies. The debris slide/boulder jumping on steep reaches triggers the debris flow of colluvium or torrent deposit along the flatter and main reaches of gullies or channels. Then two together flow like a viscous liquid with high velocities of 1-10 m/sec causing erosion *d/s*. Finally debris flow takes the shape of a fan deposit on very flat ground. The debris flow is arrested on slopes of 5° to 10° dip or by a river where landslide dams may be created if the valley is narrow.

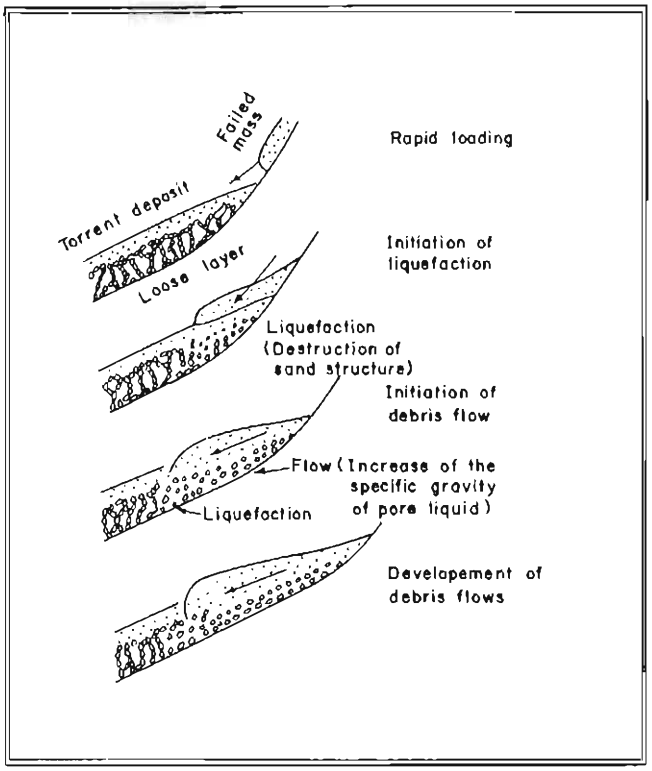


Source: Sassa 1985

**Fig. 13.2 Illustration of the Mechanism of Debris Flows**

Sassa (1985) has shown experimentally that fine particles become suspended in water (mud) because of eddy currents of rapid debris flow. Consequently, the unit weight of pore fluid (mud) rises from 1 to 1.6 gm/cc depending upon flow velocity and clay content.

Substituting in Equation 13.2, $\gamma sat$ = 1.75 *gm/cc* for loose debris, $\gamma_w$ = 1.40 *gm/cc*, the factor of safety drops to one-fifth value in dry conditions. The angle $\phi$ is now the kinetic angle of friction which is much less than the static angle of internal friction. It is because of this sudden loss of strength, which is called liquefaction, that debris flows like liquid. The fluid dynamics of debris flow are complex.

The maximum size of boulders (*d*) that will be transported by an abnormal drag force, such as sediment, is in the order of $d \approx 0.2\, v^2$ *(m)*, where *v* is the mean velocity of debris flow in m/sec. So at v=3m/sec, huge boulders of 1.8m in size would be carried like sediment.

The debris flow will be arrested at an angle of ß, according to Equation 13.2, in the shape of a debris fan (kinetic $\phi' = 25°$):

$$\tan\beta = \tan 25° \left[\frac{1.75-1.40}{1.75}\right]$$

$$\beta = 5° \ (5° - 10° \ \textit{observed}) \ .$$

The rapid debris flow can be checked by Reinforced Cement Concrete (RCC) check dams. Narrow gullies can be crossed by well-raised bridges.

### 13.3.4 *Finite Slope Failure on Curved Surface*

Many slope failures occur on curved surfaces. There are several methods of analysing such failures. These may broadly be categorized as:

- the friction-circle method and
- the method of slices

**The Friction Circle Method** (FCM) considers the total forces acting on the whole mass lying above the assumed circular surface of failure.

**The Method of Slices** (MS) involves division of the mass above an assumed failure surface into vertical slices. The slices are then analyzed statically for stability employing assumptions for avoiding indeterminate situations. The presentation is based on the work of Terzaghi and Peck which can be found in 'Slopes: Analysis and Stabilization', Transportation Research Board, 1980.

Both of these methods require determination of the critical circular slip surface. This is possible by analysing several trial surfaces and finding the slope surface which gives the least factor of safety. The critical slip surface may sometimes be determined without trial, i.e., by analytical methods.

*Chart Solution*

Hoek and Bray have prepared chart solutions based on trial slopes, circles, and methods of slices which are presented under the heading Hoek and Bray Charts for Circular Types of Failure (Fig. 13.10 to Fig. 13.14). These charts give only the static factor of safety where there are no earthquakes and no submergence of slopes.

*Computer Solution*

Package computer programmes are available to facilitate the rapid solution of stability problems involving complex and repetitive calculations. The programmes, **SARC** and **ASC,** are based on Bishop's Simple Method of slices. The Programme SARC is for the Stability Analysis of Reservoir Slopes with circular wedge mode of failure. The Programme Analysis of Slope with Circular Failure (ASC) is for determining cut slope angle. These programmes take into account earthquake forces and irregular slope surfaces also. ASC also analyses the radius of curvature of cut slope in the plan.

*General Character of Slides in Homogeneous Cohesive Soil*

A cohesive material having a shearing resistance $s = c + p \tan\phi$ can stand with a vertical slope, at least for a short time, provided the height of the slope is somewhat less than $H_c$. If the height of a slope is greater than $H_c$, the slope is not stable unless the slope angle ß is less than $90_o$. The greater the height of the slope, the smaller must be the angle ß. If the height is very great compared to $H_c$, the slope will fail unless the slope angle ß is equal to or less than $\phi - \lambda$ ($\tan\lambda$ = coefficient of the horizontal component of earthquake acceleration).

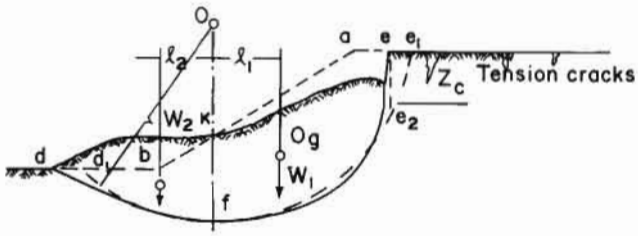


Source: Adapted from Terzaghi and Peck 1980

**Fig. 13.3 Deformation associated with slope failure**

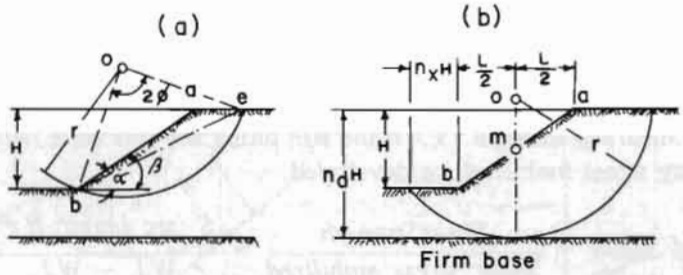


Source: Adapted from Terzaghi and Peck 1980

**Fig. 13.4 Position of critical circle for (a) Slope failure (W.Fellenius 1927) (b) Base failure**

The failure of a slope in a cohesive material is commonly preceded by the formation of a row of tension cracks behind the upper edge of the slope, as shown in Figure 13.3. Sooner or later, the opening of the cracks is followed by sliding along a curved surface, indicated by the full line in Figure 13.3. Usually, the radius of curvature of the surface of sliding is least at the upper end, greatest in the middle, and intermediate at the lower end. The curve, therefore, resembles the arc of an ellipse. If the failure occurs along a surface of sliding that intersects the slope at or above its toe (Fig. 13.4a), the slide is known as a **slope failure**. On the other hand, if the soil beneath the level of the toe of the slope is unable to sustain the weight of the overlying material, the failure occurs along a surface that passes at some depth below the toe of the slope. A failure of this type, shown in Figure 13.4b, is known as a **base failure.**

*Factor of Safety*

The Factor of Safety (F.S.) in slope analysis is generally expressed in terms of shearing strength:

$$F.S. = \frac{\textit{Shearing strength of soil } (S_r)}{\textit{Shear stress developed along failure surface}}$$

*Failed Slopes*

Failed slopes or slopes at the point of failure have a factor of safety equal to 1.0. For such slopes, we can find the shearing strength ($S_r$) of the soil along the failure surface from the geometry of the slope and the failure plane. In practice, the failure surface is located by test borings, slope borings, or deep pits.

Referring to Figure 13.3, the shearing strength of failed slope ($S_r$) is determined by:

$$W_1 l_1 = W_2 l_2 + S_r \times \text{arc } \textit{length } d_1 e_2$$

therefore,

shear stress developed = shearing resistance

$$S_r = \frac{W_1 l_1 - W_2 l_2}{\text{arc } \textit{length } d_1 e_2}$$

*Unfailed Slopes*

It is essential to know the shearing strength, $S_r$, of the soil along the probable failure plane in order to compare it with the shearing stress mobilized or developed.

$$\textit{Factory of Safety} = \frac{\textit{ShearStrength}}{\textit{Shear stress mobilized}} = \frac{S_r \text{ arc } \textit{length } d_1 e_2}{W_1 l_1 - W_2 l_2}$$

$S_r$ for cohesive and frictionless soil may be determined from unconfined compressive strength (qu) from laboratory tests. Shearing strength ($S_r$) which is referred to as the cohesion (c) for frictionless soil is roughly equal to half of the unconfined compressive strength. That is:

$$S_r = \frac{1}{2} qu = c \quad .$$

For cohesive soil with friction, shearing strength may be determined by:

$$S_r = c + p \tan\phi \quad .$$

### 13.3.5 *Soil Slope Analysis by Method of Slices*

The following discussion, extracted from Terzaghi's 'Soil Mechanics in Engineering Practice'(1980), is intended to provide a basic concept of theory behind stability analysis by the Method of Slices. Readers interested in other methods or in knowing more about slope stability may refer to any standard book on soil mechanics.

*Irregular Slopes on Non-uniform Soils* (Bishop's Simple Method)

If a slope has an irregular surface that cannot be represented by a straight line, or if the surface of sliding is likely to pass through several materials with different values of c and $\phi$, the stability can be investigated conveniently by the **method of slices**. According to this procedure, a trial circle is selected (Fig. 13.5a) and the sliding mass sub-divided into a number of vertical slices 1,2,3, etc. Each slice, such as slice 2 shown in Figure 13.5b, is acted upon by its weight W, by shear forces T and normal forces E on its sides, and by a set of forces on its base. These include the shearing force S and the normal force P. The forces on each slice, as well as those acting on the sliding mass as a whole, must satisfy the conditions of equilibrium. However, the forces T and E depend on the deformation and the stress-strain characteristics of the slide material and cannot be evaluated rigorously. They can be approximated with sufficient accuracy for practical purposes.

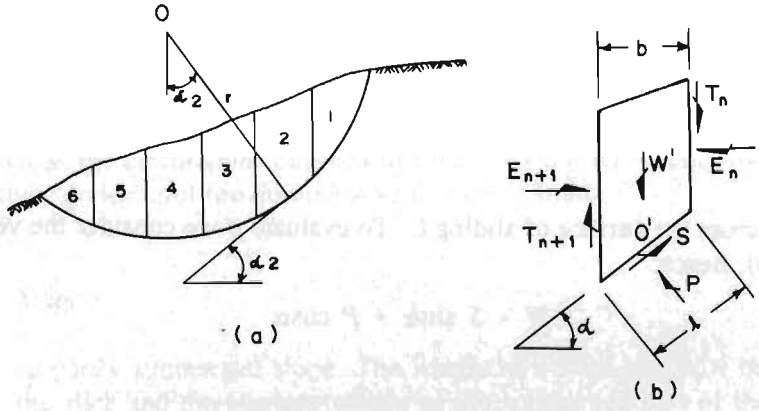


Source: adapted from Terzaghi and Peck 1980

**Figure 13.5 Method of Slices for investigating the equilibrium of a slope located above a water table**

(a) Geometry pertaining to one circular surface of sliding (b) Forces on typical slice such as slice 2 in (a)

The simplest approximation consists of setting these forces equal to zero. Under these circumstances, if the entire trial circle is located above the water table and there are no excess pore pressures, equilibrium of the entire sliding mass requires that:

$$r \sum W \sin\alpha = r \sum S \quad . \tag{13.3}$$

If $s$ is the shearing strength of the soil along $l$, then:

$$S = \frac{s}{F} l = \frac{s}{F} \frac{b}{\cos\alpha} \tag{13.4}$$

and

$$r \sum W \sin\alpha = \frac{r}{F} \sum \frac{sb}{\cos\alpha} \tag{13.5}$$

hence

$$F = \frac{\sum (\frac{sb}{\cos\alpha})}{\sum W \sin\alpha} \tag{13.6}$$

The shearing strength $s$, however, is determined by:

$$s = c + p \tan\phi$$

where,

$p$ is the normal stress across the surface of sliding $l$. To evaluate $p$ we consider the vertical equilibrium of the slice (Fig. 13.4b), hence:

$$W = S \sin\alpha + P \cos\alpha$$

and

$$p = \frac{P}{l} = \frac{P \cos\alpha}{b} = \frac{W}{b} - \frac{S}{b} \sin\alpha \quad . \tag{13.7}$$

Therefore,

$$s = c + (\frac{W}{b} - \frac{S}{b} Sin\alpha) \tan\phi = c + (\frac{W}{b} - \frac{s}{F} \tan\alpha) \tan\phi$$

and

$$s = \frac{c + (\frac{W}{b}) \tan\phi}{(1 + \frac{(\tan\alpha \tan\phi)}{F})} \tag{13.8}$$

Let

$$m_\alpha = (1 + \frac{\tan\alpha \tan\phi}{F}) \cos\alpha \tag{13.9}$$

then

$$F = \frac{\sum \frac{[c + (\frac{W}{b}) \tan\phi] b}{M_\alpha}}{\sum W \sin\alpha} \tag{13.10}$$

Equation 13.10, which gives the factor of safety $F$ for the trial circle under investigation, contains on the right-hand side the quantity $m_\alpha$ (Eq. 13.9) which is itself a function of $F$. Therefore, Equation 13.10 must be solved by successive approximations in which a value of $F = F_1$ is assumed and used for calculation of $m_\alpha$, whereupon $F$ is then computed. If the value of $F$ differs significantly from $F_1$, the calculation is repeated. Convergence is very rapid. The calculations are facilitated by the chart (Figure 13.6a) from which values of $m_\alpha$ can be taken (Janbu 1954) and by a tabular arrangement of the computations (Fig. 13.6b). In as much as the calculations outlined in Figure 13.6 refer to only one trial circle, they must be repeated for other circles until the minimum value of $F$ is found.

*Partly Submerged Slope*

Figure 13.7 shows a partly submerged slope. The weight of a slice will now be the sum of the weight of the dry part of the slice and the buoyant weight of the submerged part of this slice. It is reasonable to assume that groundwater table AA or the phreatic surface is the same as the reservoir level, at least up to the failure surface. Then there is no need to account for water pressures above and below the slices.

It is evident now that submergence reduces the toe support. Therefore, the factor of safety is reduced after submergence. In a seismic case of a partly submerged slope, the factor of safety is reduced significantly. This is because the seismic force acts upon the saturated weight of a slice and strength is mobilized by the submerged weight of the slice.

It has also been found that the factor of safety is not minimum at full reservoir level but at some critical level. Slope failure may cause turbidity currents in the reservoir eroding the valley for long distances.

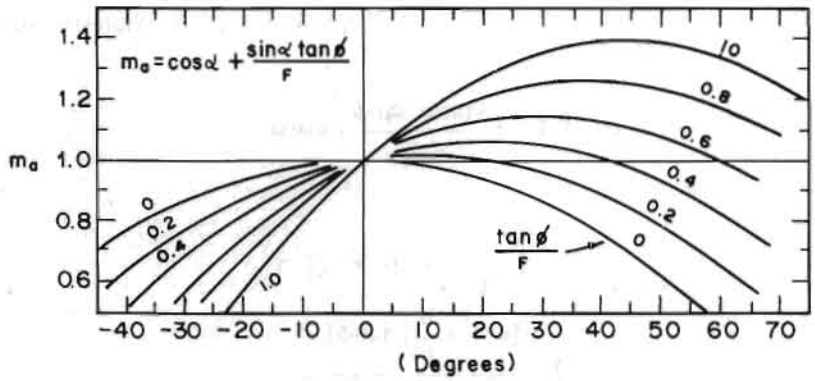


(a)

*Values from cross section*

| | 1 | 2 | 3 | 4 | 5 | 6 | 7 | 8 |
|---|---|---|---|---|---|---|---|---|
| Slice No. | $\alpha$ | sin $\alpha$ | W | W sin $\alpha$ | c + W/b tan $\phi$ | (5).b | m$\alpha$ Fa = | (6)/(7) |
| | | | | | | | | |
| | | | | | | | | $\Sigma$(8) |

*For first trial,* $F_a = \frac{\Sigma(6)}{\Sigma(4)}$ $F = \frac{\Sigma(8)}{\Sigma(4)}$

(b)

Source: adapted from Terzaghi and Peck 1980

**Fig. 13.6** **Calculation of factor of safety for slope if surface of sliding is circular and forces between slices are neglected**
(a) Chart for evaluating factor $m_\alpha$ (b) Tabular form for computation

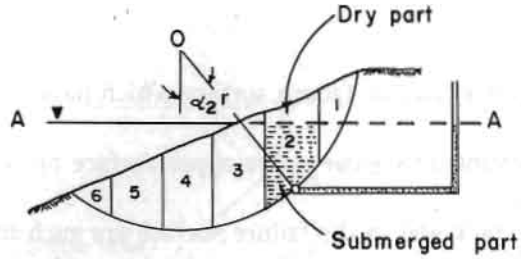


Source: adapted from Terzaghi and Peck 1980

**Fig. 13.7 Partly Submerged Slope**

*Hoek and Bray Chart for Circular Types of Failure on Slopes in Soils, Highly Jointed Rocks, and Rockfills*

These charts enable the user to carry out a rapid check on the factor of safety of a slope or upon the sensitivity of the factor of safety to changes in groundwater conditions or slope profile. The following are some considerations relating to the chart.

- Failure generally takes place in the form of a circle in the case of soils. Soils do not have strongly defined structural patterns such as unfavourably oriented seams or discontinuities in the rocks and the failure surface is free to find the line of least resistance.

- Conditions of circular failure will arise when the individual particles in a soil or rock mass are very small, compared to the size of the slope, and when these particles are interlocked as a result of their shape: hence, broken rock in a large fill tends to behave as a 'soil' and large failures will occur in a circular mode.

- Soil consisting of sand, silt, and smaller particle sizes will exhibit circular failure surfaces, even on slopes a few metres in height. It is proper to design soil slopes on the crest of highly altered and jointed rocks, on the assumption that failure would be by a circular failure process.

- The charts differ from those published by Taylor in 1948 in that they include the influence of a critical tension crack and groundwater in the slope.

- Charts may also be used for analysing rock slopes with several joint sets that are favourably oriented so that rock mass behaves like soil mass.

Derivation of Circular Failure Chart (Extracted from Hoek and Bray 1981, p. 228)

The following assumptions are made in deriving the stability charts presented in this Chapter :

a. the material forming the slope is assumed to be homogeneous, i.e., its mechanical properties do not vary with direction of loading;

b. the shear strength of the material is characterized by a cohesion c and a friction angle $\phi$ which are related by the equation $\tau = c + \sigma \tan\phi$;

c. failure is assumed to occur on a circular failure surface which passes through the toe of the slope**

d. a vertical tension crack is assumed to occur in the upper surface or on the face of the slope;

e. the locations of the tension crack and of the failure surface are such that the factor of safety of the slope is a minimum for the slope geometry and groundwater conditions considered;

f. a range of groundwater conditions, varying from a dry slope to a fully saturated slope under heavy recharge, are considered in the analysis; and

g. there is no progressive failure of the slope due to stress concentration from the toe towards the crest.

Groundwater Flow Assumptions

In order to calculate the uplift force due to water pressure acting on the failure surface and the force caused by water in the tension crack, it is necessary to assume a set of groundwater flow patterns that coincide as closely as possible with those conditions that are believed to exist in the field.

In the analysis of rock slope failures, it is normally assumed that most of the water flow takes place in discontinuities in the rock and that the rock itself is practically impermeable. In the case of slopes on soil or waste rock, the permeability of the mass material is generally several orders of magnitude higher than that of intact rock, and, hence, a general flow pattern will develop in the material behind the slope.

Within a soil mass, the equipotentials are approximately perpendicular to the **phreatic surface**. Consequently, the flow lines will be approximately parallel to the phreatic surface for the condition of **steady state drawdown**. Figure 13.8 shows that this approximation has been used for the analysis of the water pressure distribution on a slope under conditions of normal drawdown. Note that the phreatic surface is assumed to coincide with ground surface at a distance, measured in multiples of the slope height, behind the toe of the slope. This may correspond to the position of a surface water source such as a river or dam or it may simply be the point where the phreatic surface is judged to intersect the ground surface.

The phreatic surface itself has been obtained, for the range of slope angles and values of x in Figure 13.8 considered, by a computer solution of the equations proposed by Casagrande (1934), discussed in the text book by Taylor (1948). In the case of a saturated slope subjected to heavy surface recharge, the equipotentials and the associated flow lines used in the stability analysis are based upon the work of Han (1972) who used an electrical resistance analogue method for the study of groundwater flow through isotropic slopes. The charts are numbered 1 to 5 (Figure 13.10 to 13.14) to correspond with the groundwater conditions defined in Table 13.1. These charts were prepared using Bishop's Simple Method (Eq. 13.10).

---

** Terzaghi (1943) shows that the toe failure assumed for this analysis gives the lowest factor of safety provided that $\phi > 5°$. The $\phi = 0$ analysis, involving failure below the toe of the slope through the base material, has been discussed by Skempton (1948) and by Bishop (1960) and Bjerrum and is applicable to failures that occur during or after the rapid construction of an embankment slope.

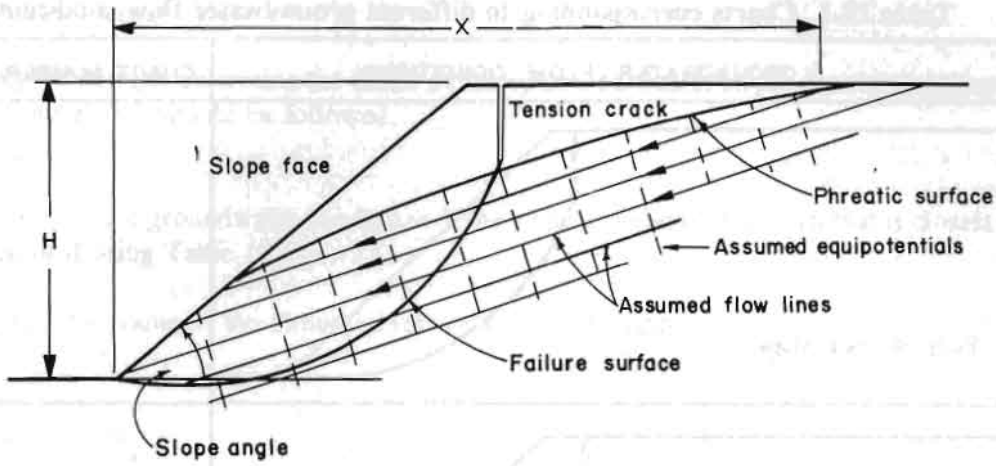


a) Groundwater flow pattern under steady state drawdown conditions where the phreatic surface coincides with the ground surface at a distance x behind the toe of the slope. The distance x is measured in multiples of the slope height H.

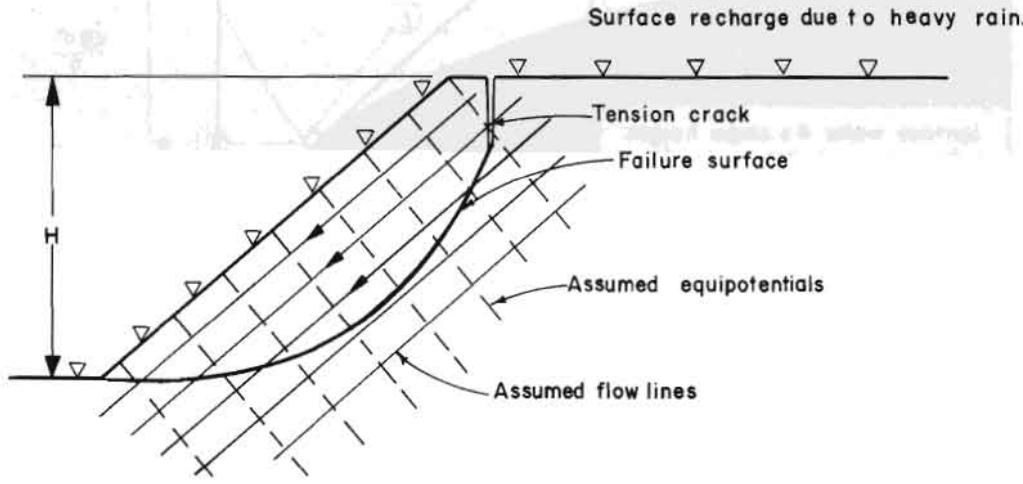


b) Groundwater flow pattern in a saturated slope subjected to heavy surface recharge by heavy rain.

Source: USDT 1981

**Fig. 13.8 Definition of groundwater flow patterns used in circular failure analysis of soil and waste rock slopes**

**Table 13.1 Charts corresponding to different groundwater flow conditions**

| GROUNDWATER FLOW CONDITIONS | CHART NUMBER |
|---|---|
| 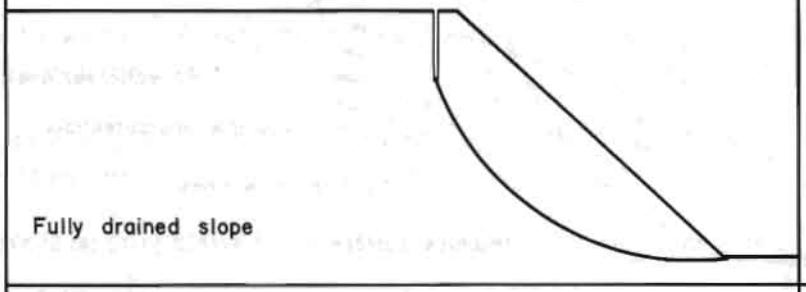  | 1 |
| 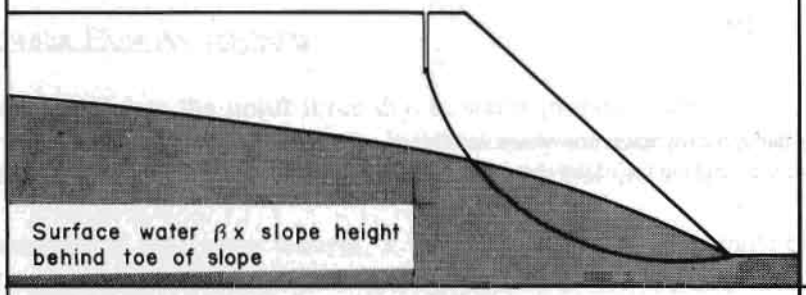  | 2 |
| 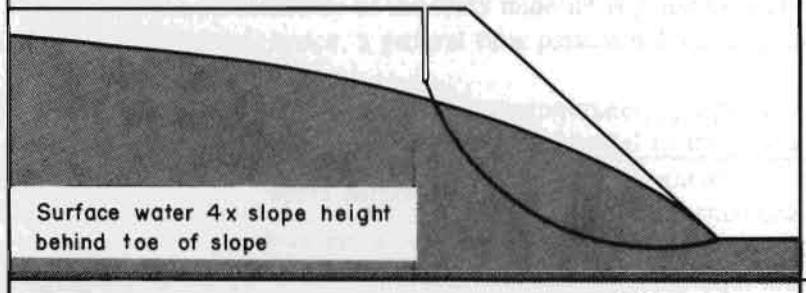  | 3 |
| 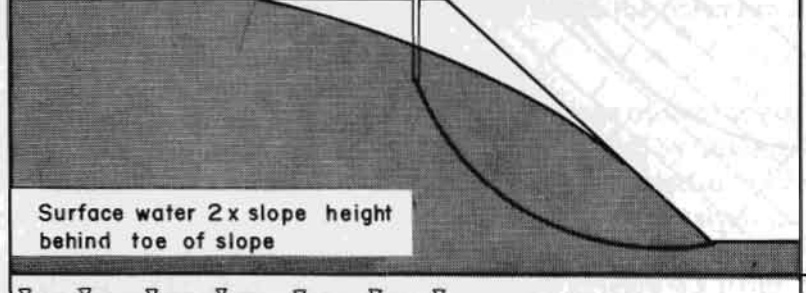  | 4 |
| 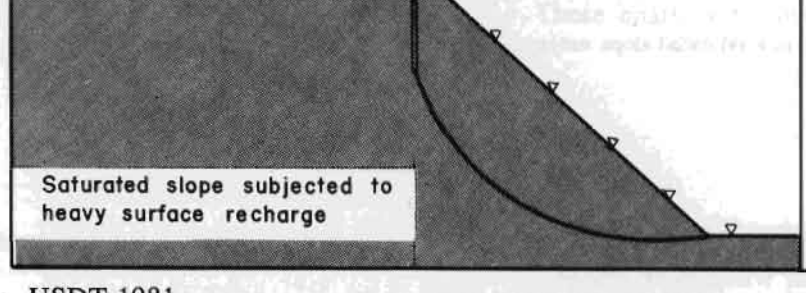  | 5 |

Source: USDT 1981

Use of the Circular Failure Charts

In order to use the charts to determine the factor of safety of a particular slope, the steps outlined below and shown in Figure 13.9 should be followed.

Step 1 : Assess upon the groundwater conditions of the slope and choose the chart that is closest to these conditions, using Table 13.1.

Step 2 : Calculate the value of the dimensionless ratio $c/\gamma H \tan\phi$.

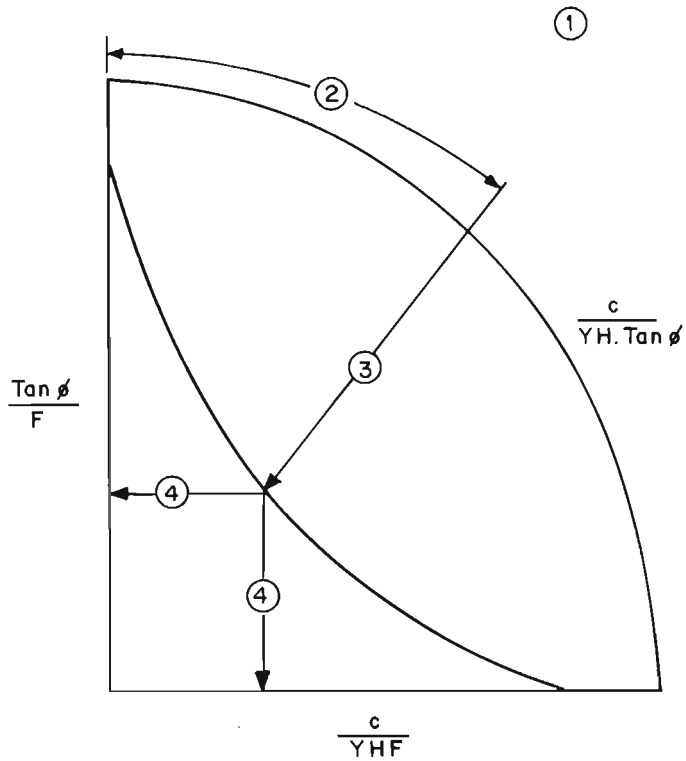


Source: USDT 1981

**Fig. 13.9 Sequence of steps in using circular failure charts to find the factor of safety**

Find this value on the outer circular scale of the chart.

Step 3 : Follow the radial line from the value found in Step 2 to its intersection with the curve that corresponds to the slope angle under consideration.

Step 4: Find the corresponding value of $Tan\phi/F$ and calculate the factor of safety.

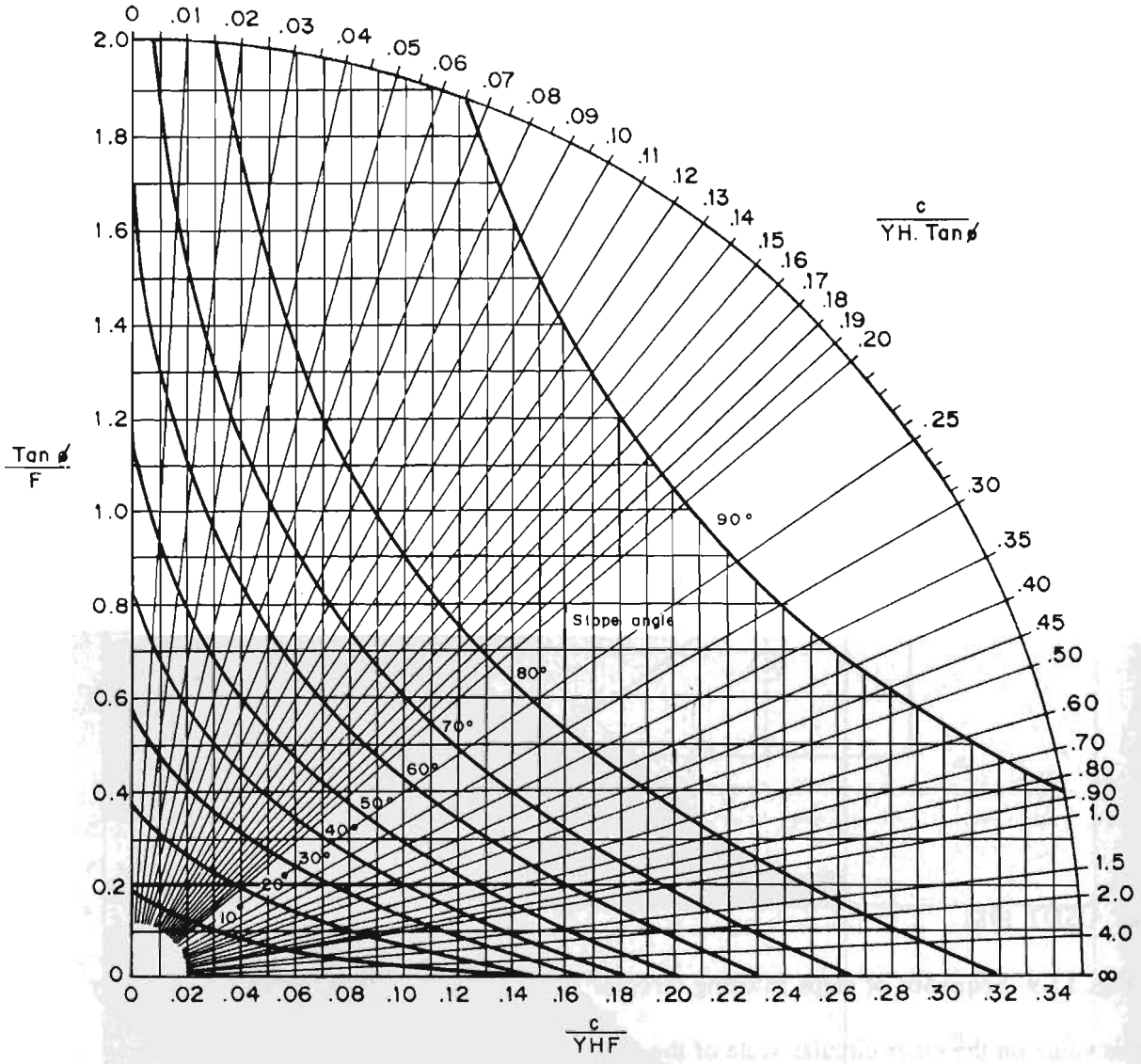


Source: USDT 1981

**Fig. 13.10 Circular failure chart number 1**

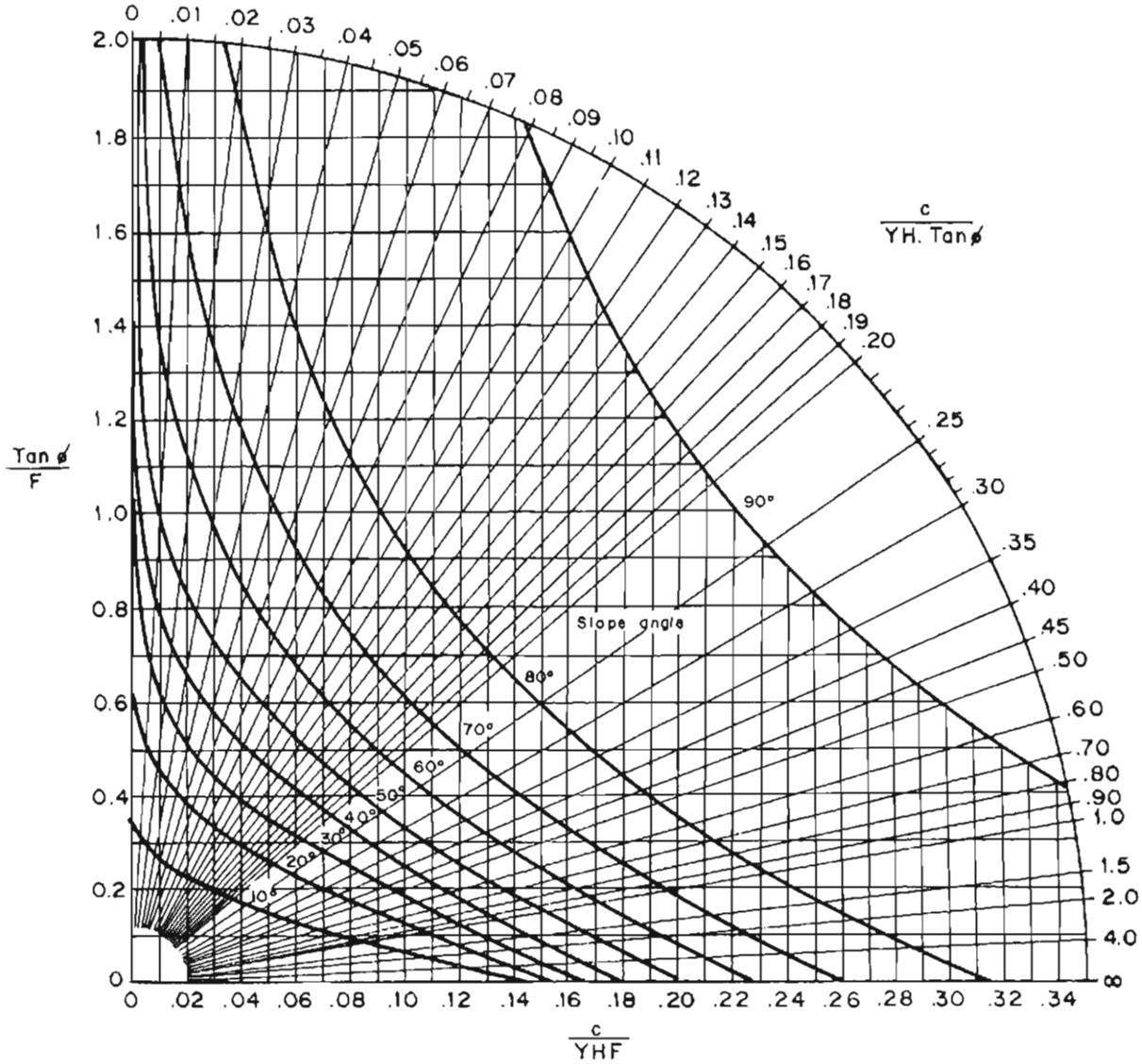


Source: USDT 1981

**Fig. 13.11 Circular failure chart number 2**

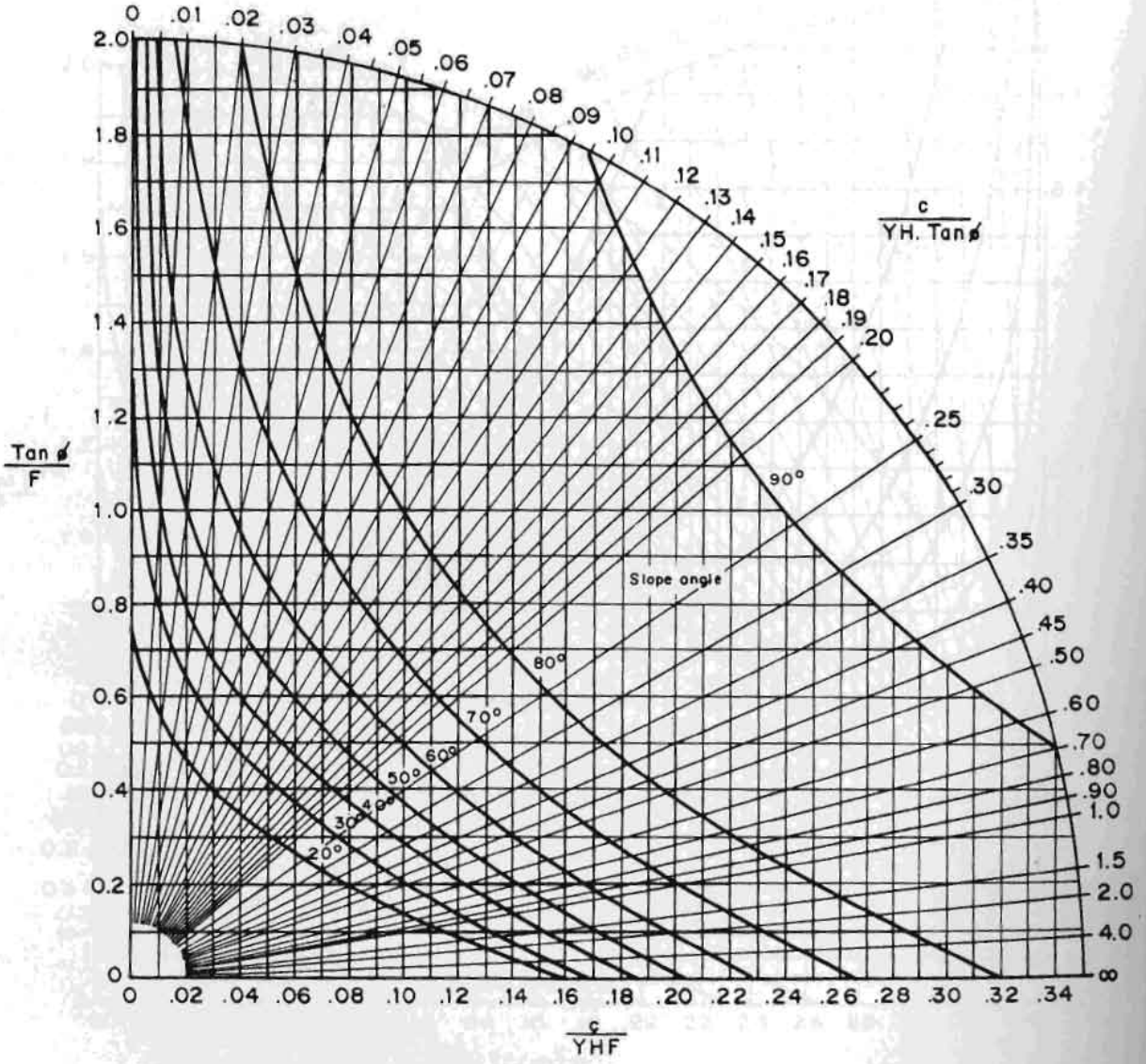


Source: USDT 1981

**Fig. 13.12 Circular failure chart number 3**

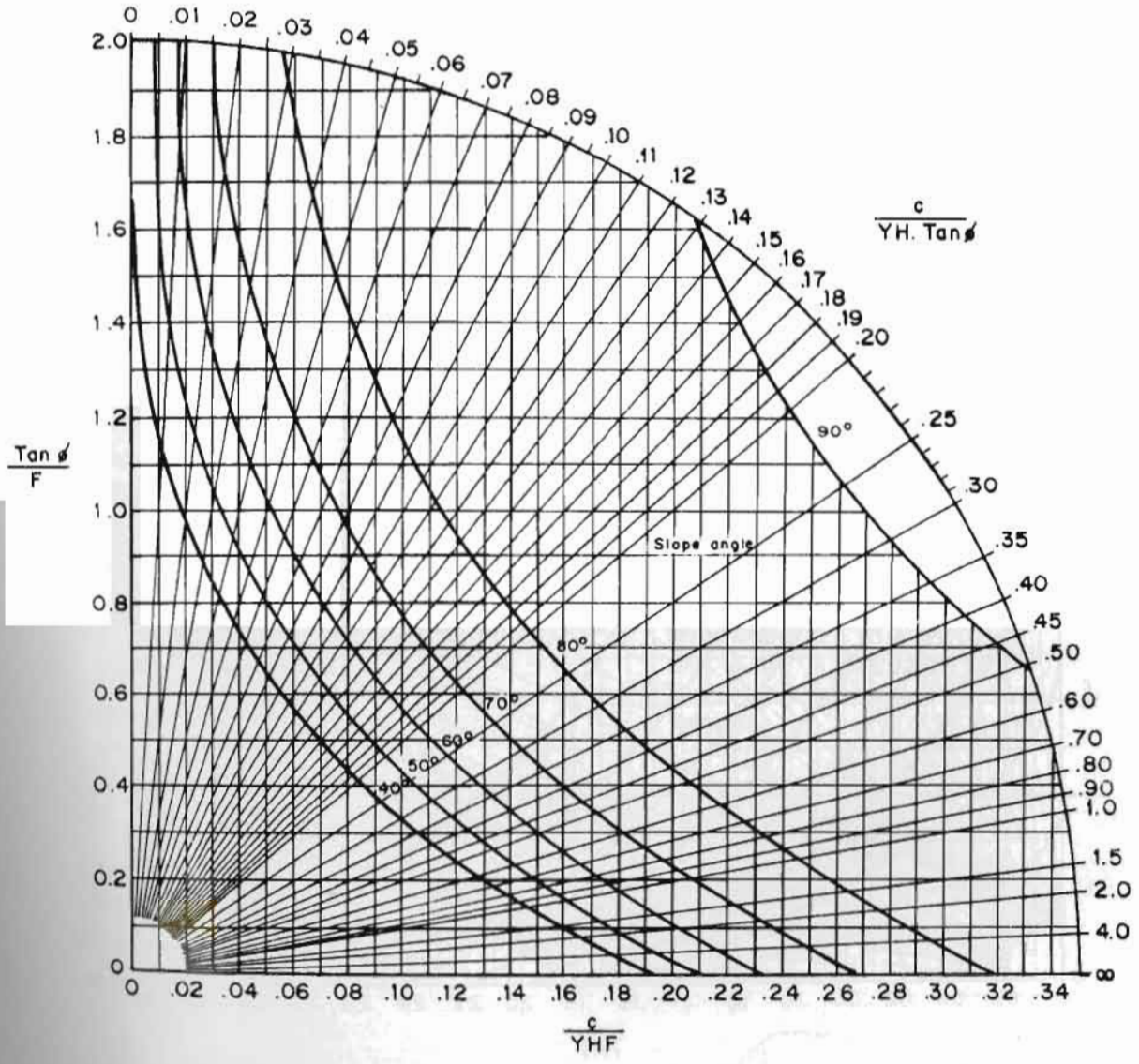


Source: USDT 1981

**Fig. 13.13 Circular failure chart number 4**

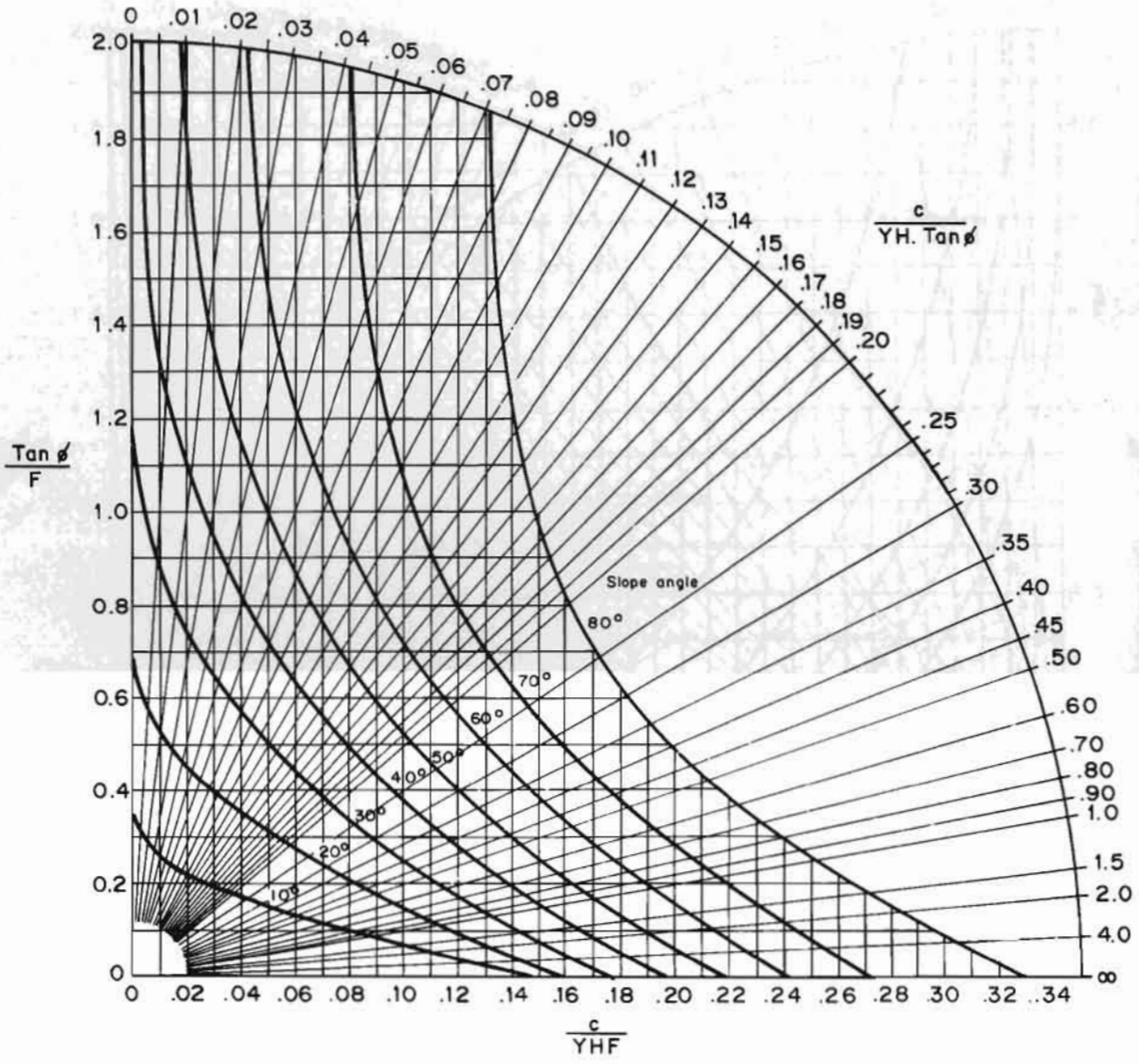


Source: USDT 1981

**Fig. 13.14 Circular failure chart number 5**

*Examples*

1) A 15 m high slope with a face angle of 40° is to be excavated in overburdened soil with a density = 1.6t/m², a cohesive strength of 3.9 t/m² and a friction angle of 30°. Find the factor of safety of the slope, assuming that there is a surface water source 60 m behind the toe of the slope.

   The groundwater conditions indicate the use of Chart No. 3. The value of $c/(\gamma\ H\ Tan\phi) = 0.28$ and the corresponding value of $Tan\ \phi/F$, for a 40° slope, is 0.32. Hence, the factor of safety of the slope is 1.80.

2) China Clay Pit Slope.*** Ley (1972) has investigated the stability of a China clay pit slope which was considered to be potentially unstable. The slope profile is illustrated in Figure 13.15 and the input data used for the analysis is included in this figure. The material, a heavily kaolinized granite, was carefully tested by Ley and the friction angle and cohesive strength are considered reliable for this particular slope.

   Two piezometers on the slope, and a known water source some distance behind the slope, enabled Ley to postulate the phreatic surface shown in Figure 13.15. The chart that corresponds most closely to these groundwater conditions is considered to be Chart Number 2. From the information given in Figure 13.15 the value of the ratio $c/(\gamma\ H\ Tan\phi) = 0.0056$ and the corresponding value of Tan $\phi$/F, from Chart Number 2, is 0.76. Hence, the factor of safety of the slope is 1.01. Ley also carried out a number of trial calculations using Janbu's Method (1954) and, for the critical slip circle shown in Figure 13.15, found a factor of safety of 1.03. These factors of safety indicate that the stability of the slope was inadequate under the assumed conditions and steps were taken to deal with the problem.

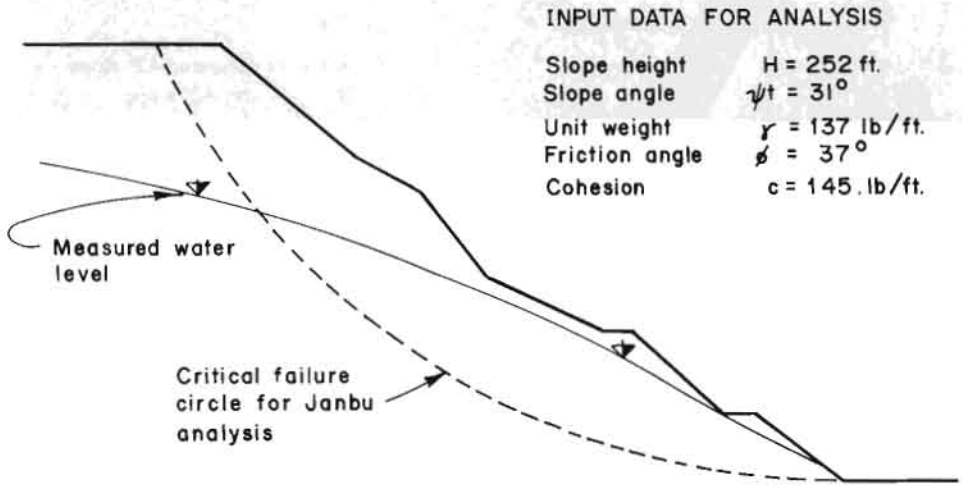


Source: USDT 1981

**Fig. 13.15 Slope profile of china clay pit slope considered in example number 2**

*** This section is extracted from Hoek and Bray 1981, p. 242.

3) Projected Highway Slope. A highway plan calls for a slope on one side of the highway having an angle of 42°. The total height of the slope will be 200ft when completed and it is required to check whether the slope will be stable. A site visit enables the slope engineer to assess whether the slope consists of weathered and altered material and whether failure, if it occurs, will be of a circular type. Insufficient time is available for groundwater levels to be accurately established or for shear tests to be carried out. The stability analysis is carried out as follows.

For the condition of limiting equilibrium, F=1 and Tan$\phi$/F = Tan $\phi$. For a range of friction angles, the values of Tan$\phi$ are used to find the values of $c/(\gamma\ H\ Tan\phi)$, for $42^0$, by reversing the procedure outlined in Figure 13.9. The value of the cohesion $c$, which is mobilized at failure, for a given friction angle, can then be calculated. These analyses are carried out for dry slopes, using Chart 1, and for saturated slopes, using Chart 5. The resulting range of friction angles and cohesive strengths that would be mobilized at failure are plotted in Figure 13.16 (back analysis of a slope with circular wedge failure is easily performed with the computer programme BASC).

The shaded circle included in Figure 13.16 indicates the range of shear strengths to be considered probable for the material under consideration. It is clear from this figure that the available shear strength may not be adequate to maintain stability on this slope, particularly when the slope is saturated. Consequently, the slope engineer would have to recommend that either the slope should be flattened or that investigations into the groundwater conditions and material properties should be undertaken in order to establish whether the analysis presented in Figure 13.16 is too pessimistic.

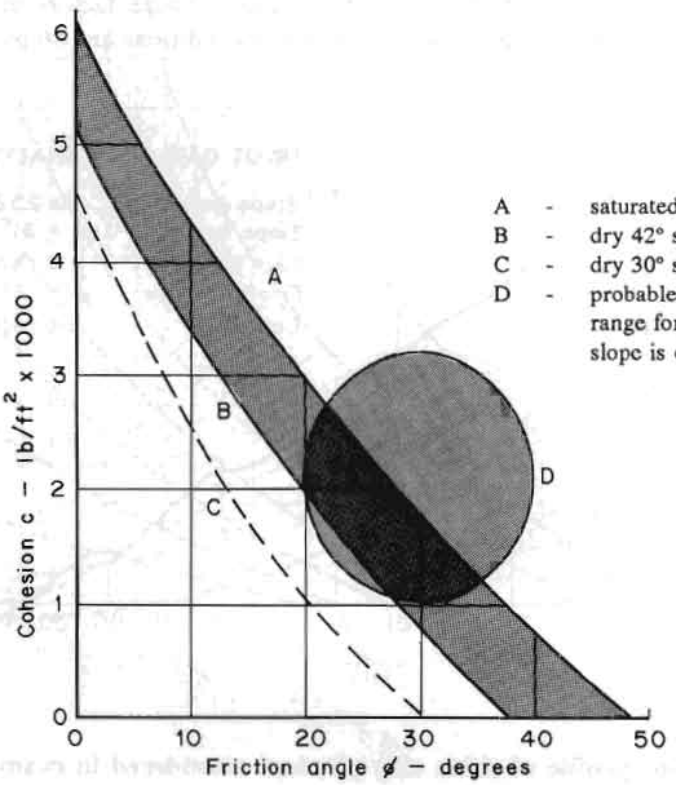


Source: USDT 1981

**Fig. 13.16** **Comparison between shear strength mobilized and shear strength available for the slope considered in example number 3**

The effect of flattening the slope can be checked very quickly by finding the value of $c/(\gamma H \, Tan\phi)$ for a flatter slope, say 30°, using the same method as for the 42° slope. The dashed line in Figure 13. 16 indicates the shear strength that would be mobilized in a dry slope with a face angle of 30°.

*Composite Surface Sliding*

In many instances, the geometric or geologic conditions of the slope are such that the surface of sliding may not be even approximately circular. For these conditions, the Method of Slices can be extended (Janbu 1954 and Nouveiller 1965).

If the subsoil contains one or more thin exceptionally weak seams, the sliding surface is likely to consist of three or more sections that do not merge smoothly one into another. In stability computations such a surface cannot be replaced by a continuous curve without the introduction of an error on the unsafe side.

Figure 13.17 represents a slope underlain by a thin layer of very soft clay with cohesion *C*. If such a slope fails, the slip occurs along any composite surface *abcd*. In the right-hand part of the sliding mass, represented by the area *abf*, active failure must be expected because the earth stretches horizontally under the influence of its own weight. The central part, *bcef*, moves to the left under the influence of the active pressure on *bf*. The left-hand part of the sliding mass, *cde*, experiences passive failure due to the thrust of the advancing central part, *bcef*.

Analysis of the failure is quite complicated. Hence experts in geotechnical engineering should be consulted for computing factors of safety. The computer programme SANC is also available for Stability Analysis of Slopes with Non-vertical Slices and Non-circular Slip Surfaces. Unlike the programme developed by Hoek, SANC converges rapidly into a realistic value of factors of safety and inter-slice forces.

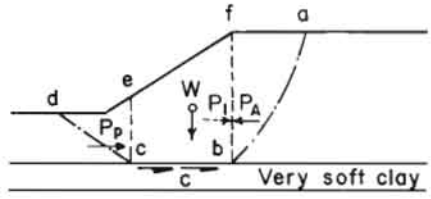


**Fig. 13.17 Failure of slope underlain by thin layer of very soft clay**

## 13.4 ROCK SLOPE STABILITY

As already discussed, failure in the soil may occur along a plane surface or curved surface. The plane failure, also called translational failure, may be in the form of debris flow or debris slide while failure along a curved surface is in the form of slumping. A major slide may be complex involving all the three conditions of flow, debris slide, and slumping.

Failures on rock slopes are in the form of planar slides, wedge slides, and topples or rockfalls. Almost all these failures are associated with existing discontinuities or joints resulting from weathering, gravitational, and tectonic forces: in many instances they are facilitated by surface and sub-surface water.

For most problems of rock slopes, the simple approach discussed in the following sections may be adequate. Analysis of a large area with several discontinuities requires the use of stereo plots. The computer programmes, Stability Analysis of Rock Slope with Plane Wedge Failure (SASP) and to determine the Factor of Safety of a Tetrahydral Wedge with Horizontal Slope Crest and with No Tension crack (SASW), based on Hoek and Bray (1981), for plane and wedge analysis may be used. The SASW Programme is for Stability Analysis of Slopes with Wedge Failure. The SASP Programme is for determining cut slope angle. These programmes take into account earthquake forces, water pressure, and submergence. The following sections aim to provide the fundamental concepts of plane and wedge slide analysis. These are based on Hoek and Bray and are extracted from "Rock Slopes" - a manual published by the United States Department of Transportation (USDT), Federal Highway Association (FHA), 1981.

### 13.4.1 *Plane Failure*

*Introduction*

A plane failure is a comparatively rare phenomenon in rock slopes because it is only occasionally that all the geometrical conditions required to produce such a failure occur in an actual slope. The wedge type of failure is a much more general case and many rock slope engineers treat the plane failure as a special case of the more general wedge failure analysis.

While this is probably the correct approach for the experienced slope designer, who has a wide range of design tools at his disposal, it would not be right to ignore the two-dimensional case in this general discussion on slope failure. There are many valuable lessons to be learned from a consideration of the mechanics of this simple failure mode and it is particularly useful for demonstrating the sensitivity of the slope to changes in shear strength and groundwater conditions - changes that are less obvious when dealing with the more complex mechanics of a three-dimensional slope failure.

*General Conditions for Plane Failure*

For sliding to occur on a single plane, the following geometrical conditions must be present (Fig. 13.18).

a. The plane on which sliding occurs must strike parallel or nearly parallel (within approximately 20°) to the slope face.

b. The failure plane must 'daylight' on the slope face. This means that its dip must be smaller than the dip of the slope face, i.e., $\psi_f > \psi_p$.

c. Release surfaces that provide negligible resistance to sliding must be present in the rock mass to define lateral boundaries of the slide. Alternatively, failure can occur on a failure plane passing through the convex 'nose' of a slope.

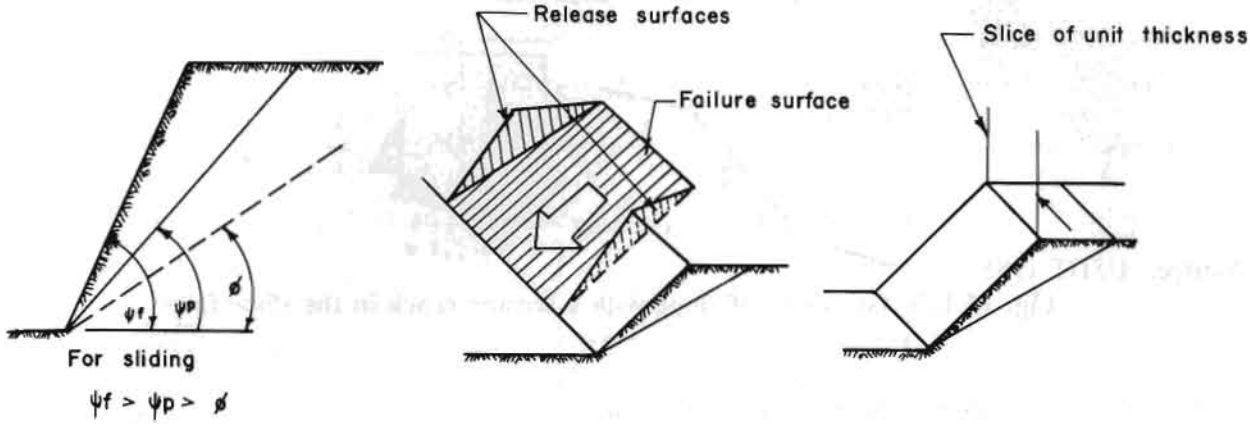


Source: USDT 1981

**Figure 13.18 Plane failure**

In analyzing two-dimensional slope problems, it is usual to consider a slice of unit thickness taken at right angles to the slope face. This means that the area of the sliding surface can be represented by the length of the surface visible on a vertical section, although the slope and the volume of the sliding block are represented by the area of the figure representing this block on the vertical section.

*Plane Failure Analysis*

The geometry of the slope considered in this analysis is defined in Figure 13.19. Note that two cases must be considered.

A. A slope having a tension crack on its upper surface.
B. A slope with a tension crack in its face.

The transition from one case to another occurs when the tension crack coincides with the slope crest, i.e., when:

$$Z/H = (1 - \cot \psi_f \,.\, Tan\, \psi_p) \quad . \tag{13.11}$$

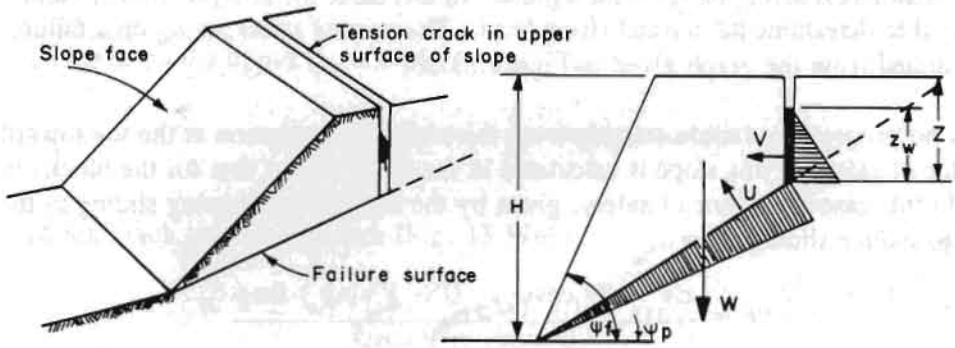


Source: USDT 1981

**Fig. 13.19a Geometry of a slope with a tension crack on the upper slope surface**

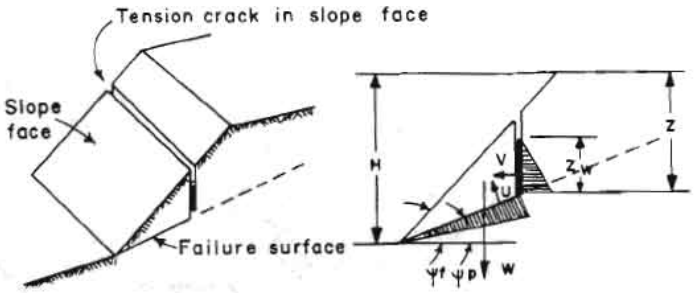


Source: USDT 1981

**Fig. 13.19b Geometry of slope with a tension crack in the slope face**

The following assumptions are made in this analysis:

a. Both sliding surface and tension crack strike parallel to the slope surface.

b. The tension crack is vertical and is filled with water to a depth *Zw*.

c. Water enters the sliding surface along the base of the tension crack and seeps along the sliding surface, escaping at atmospheric pressure where the sliding surface daylights on the slope face. The pressure distribution induced by the presence of water in the tension crack and along the sliding surface is illustrated in Figure 13.19. It is assumed that the slope is not covered by snow or clay.

d. The forces *W* (the weight of the sliding block), *U* (uplift force caused by water pressure on the sliding surface), and *V* (force caused by water pressure in the tension crack) all act through the centroid of the sliding mass. In other words, it is assumed that there are no moments that would tend to cause rotation of the block and hence failure is by sliding only. While this assumption may not be strictly true for actual slopes, the errors introduced by ignoring moments are small enough to neglect. However, on steep slopes with steeply dipping discontinuities, the possibility that toppling failure may occur should be kept in mind.

e. The shear strength of the sliding surface is defined by cohesion *c* and a friction angle $\phi$ which are related by the equation $\tau = c + \sigma \tan\phi$. In the case of a rough surface having a curvilinear shear strength curve, the apparent cohesion and apparent friction angle, defined by a tangent to the curve, are used. This tangent should touch the curve at a normal stress value which corresponds to the normal stress acting on the failure plane. In this case, the analysis is only valid for the slope height used to determine the normal stress level. The normal stress acting on a failure surface can be determined from the graph given in Figure 13.20.

f. There is no progressive failure starting from the stress concentration at the toe towards the crest. The factor of safety of this slope is calculated in the same way as that for the block on an inclined plane. In this case the factor of safety, given by the total force resisting sliding to the total force tending to induce sliding, is:

$$F = \frac{cA + (W.\cos\psi_p - U - V.\sin\psi_p)\tan\phi}{W.\sin\psi_p + V.\cos\psi_p} \qquad (13.12)$$

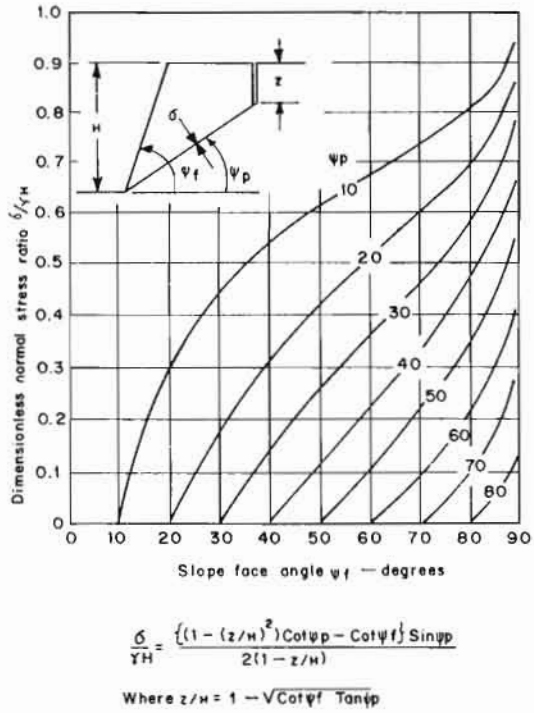


Source: USDT 1981

**Fig. 13.20 Normal stress acting on the failure plane on a rock slope**

where, from Figure 13.19:

$$A = (H-Z).\text{cosec}\ \psi_p \quad . \tag{13.13}$$

$$U = \frac{1}{2}\ \gamma_w.Z_w(H-Z).\text{cosec}\ \psi_p \quad . \tag{13.14}$$

$$V = \frac{1}{2}\ \gamma_w.Z^2\ W \quad . \tag{13.15}$$

For the tension crack on the upper slope surface (Fig. 13.19a)

$$W = \frac{1}{2}\ \gamma H^2\ [(1-\frac{Z}{H})^2\ \cot\psi_p\ -\ \cot\psi_f] \tag{13.16}$$

and for the tension crack in the slope face (Fig. 13.19b)

$$W = \frac{1}{2}\ \gamma H^2\ [(1-\frac{Z}{H})^2\ \cot\psi_p\ (\cot\psi_p.\tan\psi_f\ -\ 1)] \quad . \tag{13.17}$$

*Influence of Groundwater on Stability*

In the preceding discussion it has been assumed that it is only the water present in the tension crack and the water along the failure surface that influence the stability of the slope. This is equivalent to assuming that the rest of the rock mass is impermeable, an assumption that is certainly not always justified. Consideration must, therefore, be given to water pressure distribution;other than that upon which the analysis so far presented has been based.

The current state of knowledge in rock engineering does not permit a precise definition of the groundwater flow patterns in a rock mass. Consequently, the only possibility open to the slope designer is to consider a number of realistic extremes in an attempt to bracket the range of possible factors of safety and to assess the sensitivity of the slope to variations in groundwater conditions.

a. Dry Slopes

The simplest case which can be considered is that in which the slope is assumed to be completely drained. In practical terms, this means that there is no water pressure in the tension crack or along the sliding surface. Note that there may be moisture in the slope but, as long as no pressure is generated, it will not influence the stability of the slope. Under these conditions, the forces V and U are both zero and equation 13.12 reduces to:

$$F = \frac{c.A}{W.\sin\psi_p} + \cot\psi_p.\tan\phi \quad . \tag{13.18}$$

b. Water in Tension Crack and on Sliding Surface

These are the conditions that were assumed in deriving the general solution presented on the preceding pages. The pressure distribution along the sliding surface has been assumed to decrease linearly from the base of the tension crack to the intersection of the failure surface and the slope face. This water pressure distribution is probably very much simpler than that which occurs on an actual slope but, since the actual pressure distribution is unknown, this assumed distribution is as reasonable as any other that can be made.

It is possible that a more dangerous water pressure distribution could exist if the face of the slope became frozen in winter so that, instead of the zero pressure condition which has been assumed at the face, the water pressure at the face would be that caused by the full head of water in the slope. Such extreme water pressure conditions may occur from time to time and the slope designer should keep this possibility in mind. However, for general slope design, the use of this water pressure distribution would result in an excessively conservative slope and hence the triangular pressure distribution used in the general analysis is presented as the basis for normal slope design.

In the case of partly submerged rock slopes, it is found that the factor of safety is slightly increased as the effective weight of the plane wedge is reduced. However in seismic cases, the factor of safety is likely to decrease.

c. Saturated Slope with Heavy Recharge

If the rock mass is heavily fractured, so that it becomes relatively permeable, a groundwater flow pattern similar to that which would develop in a porous system could occur. The most dangerous conditions that would develop in this case would be those created by prolonged heavy rainfall.

Flow nets for saturated slopes with heavy surface recharge have been constructed and the water pressure distributions obtained from these flow nets have been used to calculate the factors of safety of a variety of slopes. The process involved is too lengthy to include in this chapter, but the results can be summarized in a general form. It has been found that the factor of safety for a permeable slope, saturated by heavy rain and subjected to surface recharge by continued rain, can be approximated by Equation 13.12 assuming that the tension crack is water-filled, i.e., $Z_w = Z$.

In view of the uncertainties associated with the actual water pressure distributions, which could occur in rock slopes subjected to these conditions, this analysis has not been further refined here.

*Critical Tension Crack Depth*

In the analysis that has been presented, it has been assumed that the position of the tension crack is known from its visible trace on the upper surface or on the face of the slope and that its depth can be established by constructing an accurate cross-section of the slope. When the tension crack position is unknown, because, for example, of the presence of soil on the top of the slope, it becomes necessary to consider the most probable position of a tension crack.

The influence of tension crack depth, and of the depth of water in the tension crack, upon the factor of safety of a typical slope is illustrated in Figure 13.21.

When the slope is dry or nearly dry, the factor of safety reaches a minimum value that, in the case of the example considered, corresponds to a tension crack depth of 0.42H. This critical tension crack depth for a dry slope can be found by minimizing the right-hand side of Equation 13.18 with respect to Z/H.

This gives the critical tension crack depth as:

$$\frac{Z_c}{H} = 1 - \sqrt{\cot\psi_f \tan\psi_p} \quad . \tag{13.19}$$

From the geometry of the slope (Fig. 13.19) the corresponding position of the tension crack is:

$$\frac{b_c}{H} = \sqrt{\cot\psi_f \cot\psi_p} - \cot\psi_f \quad . \tag{13.20}$$

Figure 13.21 shows that, once the water level $Z_w$ exceeds about one quarter of the tension crack depth, the factor of safety of the slope does not reach a minimum until the tension crack is water-filled. In this case, the minimum factor of safety is given by a water-filled tension crack which is coincident with the crest of the slope (b=0).

It is most important, when considering the influence of water in a tension crack, to consider the sequence of tension crack formation and water filling. Field observations suggest that tension cracks usually occur

behind the crest of a slope and, from Figure 13.21, it must be concluded that these tension cracks occur as a result of movement in a dry or nearly dry slope. If this tension crack becomes water-filled, as the result of a subsequent rainstorm, the influence of the water pressure will be in accordance with the rules laid down earlier in this chapter. The depth and location of the tension crack are, however, independent of the groundwater conditions and are defined by Equations 13.19 and 13.20.

If the tension crack forms during heavy rain, or if it is located on a pre-existing geological feature such as a vertical joint, Equations 13.19 and 13.20 no longer apply. In these circumstances, when the tension crack position and depth are unknown, the only reasonable procedure is to assume that the tension crack is coincident with the slope crest and that it is water-filled. It may be noted that Equation 13.19 predicts the ratio of depth of tension crack and slope height to be unity for vertical slopes or cuts. In fact, this ratio is seldom more than 0.5.

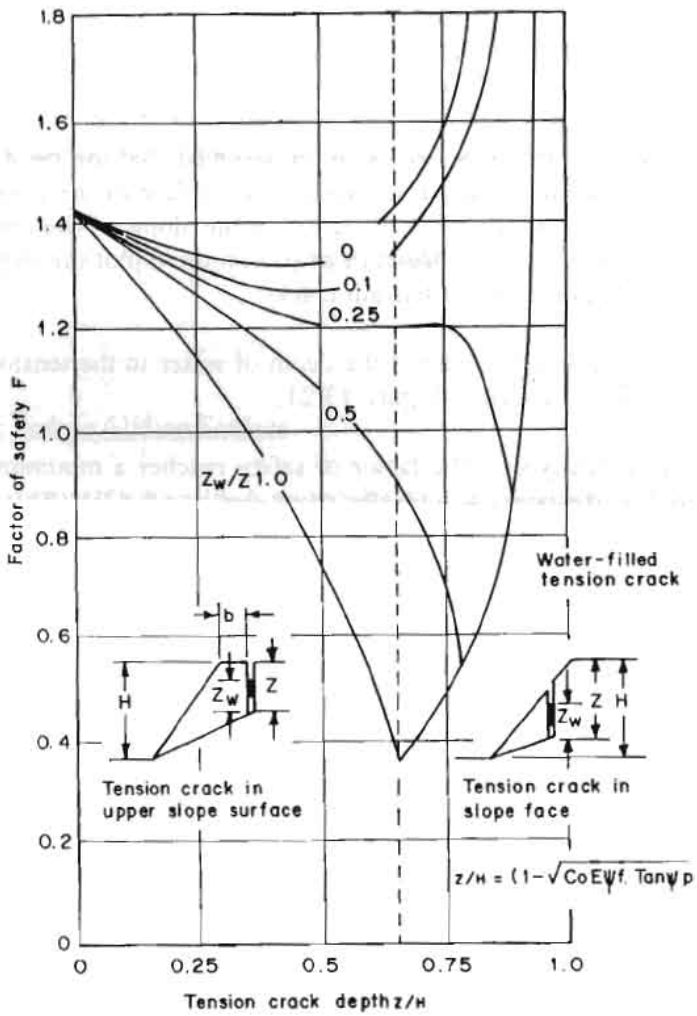


Source: USDT 1981

**Fig. 13.21 Influence of tension crack depth and of depth of water in the tension crack upon the factor of safety of a slope**

*The Tension Crack as An Indicator of Instability*

Anyone who has examined excavated rock slopes cannot have failed to notice the frequent occurrence of tension cracks on the upper surfaces of these slopes. Some of these cracks have been visible for a number of years and, in many cases, do not appear to have had any adverse influence upon the stability of the slope. It is, therefore, interesting to consider how such cracks are formed and whether they can give any indication of slope instability.

In a series of very detailed model studies on the failure of slopes in jointed rocks, Barton (Barton and Chaubey 1977) found that the tension crack was generated as a result of small shear movements within the rock mass. Although these individual movements were very small, their cumulative effect was a significant displacement of the slope surfaces - sufficient to cause separation of vertical joints behind the slope crest and to form 'tension' cracks. The fact that the tension crack is caused by shear movements in the slope is important because it suggests that it must be assumed that shear failure initiated within the rock mass.

It is impossible to quantify the seriousness of this failure since it is only the start of a very complex progressive failure process about which very little is known. It is quite probable that, in some cases, the improved drainage resulting from the opening up of the rock structure, and the interlocking of individual blocks within the rock mass, could give rise to an increase in stability. In other cases, the initiation of failure could be followed by a very rapid decrease in stability with consequent failure of the slope.

In summary, Hoek and Bray 1981 recommend that the presence of a tension crack should be taken as an indication of potential instability and that, in the case of an important slope, this should signal the need for detailed investigation into the stability of that particular slope.

*Critical Failure Plane Inclination*

When a through-going discontinuity,such as a bedding plane,exists in a slope and the inclination of this discontinuity is such that it satisfies the conditions for plane failure, the failure of the slope will be controlled by this feature. However, when no such feature exists and when a failure surface, if it were to occur, would follow minor geological features and, in some places, would pass through intact material, how could the inclination of such a failure path be determined?

The first assumption that must be made concerns the shape of the failure surface. On a soft rock slope, or a soil slope with a relatively flat slope face ($\psi_f < 45°$), the failure surface would have a circular shape. The analysis of such failure surfaces will be dealt with as for soils.

In steep rock slopes, the failure surface is almost planar and the inclination of such a plane can be found by partial differentiation of Equation 13.12 with respect to $\psi_p$ and by equating the resulting differential to zero. For dry slopes this gives the critical failure plane inclination $\psi_{pc}$ as:

$$\psi_{pc} = \frac{1}{2}(\psi_f + \phi) \quad . \tag{13.21}$$

The presence of water in the tension crack will cause the failure plane inclination to be reduced by up to 10 per cent and, in view of the uncertainties associated with this failure surface, the added complication

of including the influence of groundwater is not considered justified. Consequently, Equation 13.21 can be used to obtain an estimate of the critical failure plane inclination on steep slopes which do not contain through-going discontinuity surfaces.

*Influence of Undercutting of the Toe of a Slope*

It is not unusual for the toe of a slope to be undercut, either intentionally by excavation or by natural agencies such as the weathering of underlying soft strata or, in the case of sea cliffs, by the action of waves. The influence of such undercutting on the stability of a slope is important in many practical situations and an analysis of this stability is presented here.

In order to generalise the solution, it is assumed that the geometry of the slope is that illustrated in Figure 13.22. A previous failure is assumed to have left a face inclined at $\psi_f$ and a vertical tension crack depth $Z_1$. As a result of an undercut of $\Delta M$, inclined at an angle $\psi_o$, a new failure occurs on a plane inclined at $\psi_p$ and involves the formation of a new tension crack of depth $Z_2$.

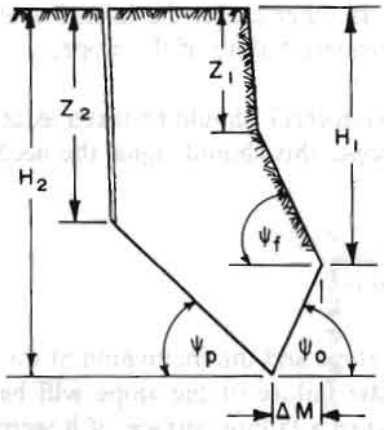


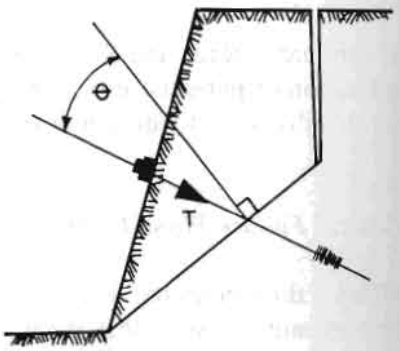


Source: USDT 1981

**Fig. 13.22a Geometry of undercut slope**

**Fig. 13.22b Reinforcement of a slope**

The factor of safety of this slope is given by Equation 13.12 but it is necessary to modify the expression for the weight terms as follows:

$$W = \frac{1}{2}\gamma[(H_2^2 - Z_2^2)\cot\psi_p - (H_1^2 - Z_1^2)\cot\psi_f + (H_1 + H_2)\Delta M] \quad . \tag{13.22}$$

Note that, for $\psi_o > 0$,

$$\Delta M = (H_2 - H_1)\cot\psi_o \quad . \tag{13.23}$$

The critical tension crack depth for a dry undercut slope is:

$$Z_2 = \frac{c.\cos\ \phi}{\gamma\ \cos\ \psi_p.\sin\ (\psi_p\ -\ \phi)} \quad . \tag{3.24}$$

*Reinforcement of a Slope*

When it has been established that a particular slope is unstable, it becomes necessary to consider whether it is possible to stabilize the slope by drainage or by the application of external loads. Such external loads may be applied by the installation of rock bolts or cables anchored into the rock mass behind the failure surface or by the construction of waste rock berm to support the toe of the slope.

The factor of safety of a slope, with external loading of magnitude T, inclined at an angle Θ to the failure plane as shown in the Figure 13.22b is approximated by:

$$F = \frac{cA\ +\ (W.\cos\ \psi_p\ -\ U\ -\ V.\sin\ \psi_p\ +\ T.\cos\theta)\ \tan\phi}{W.\sin\ \psi_p\ +\ V.\cos\ \psi_p\ -\ T.\sin\theta} \quad . \tag{13.25}$$

This equation is correct for the condition of limiting equilibrium (F=1) but there are certain theoretical problems in using it for other values of F.

*Computer Programmes*

The following programmes are available for rapid computation of factors of safety and design of remedial measures:

(i) SASP is for the stability analysis of slopes with plane wedge failure. It also gives designs of drainage systems and/or rock anchor systems as the situation demands.

(ii) SARP is for the stability analysis of reservoir slopes with plane wedge failure.

(iii) ASP is for determining cut slope angle of slope with plane wedge failure. It accounts for the radius of slope curvature in the plan.

(iv) BASP is for the back analysis of slopes with plane wedge failure.

All programmes take earthquake forces and the non-linear strength criteria of Barton into account.

### 13.4.2 *Wedge Failure*

*Introduction*

The previous section was concerned with slope failure resulting from sliding on a single planar surface

dipping into the excavation and striking parallel, or nearly parallel, to the slope face. It was stated that the plane failure analysis is valid provided that the strike of the failure plane is within 20° of the strike of the slope face. This section is concerned with the failure of slopes in which there are structural features upon which sliding can occur and strike across the slope crest and where sliding takes place along the line of intersection of two such planes.

In this section, the basic mechanics of failure, involving the sliding of a wedge along the line of intersection of two planar discontinuities, are presented in a form that the non-specialist reader should find easy to follow. Unfortunately the very simple equations which are presented to illustrate the mechanics are of limited practical value because the variables used to define the wedge geometry cannot easily be measured in the field.

Consequently, the second part of this section deals with stability analysis in terms of the dips and dip directions of the planes and the slope face. In the transformation of the equations, which is necessary in order to accommodate this information, the basic mechanics become obscure but it is hoped that the reader will be able to follow the logic involved in the development of these equations.

In this section, discussion is limited to the case of the sliding of a simple wedge acted upon by friction, cohesion, and water pressure. The influence of a tension crack and of external forces because of bolts, cables, or seismic accelerations result in a significant increase in the complexity of the equations and, since it would only be necessary to consider these influences on the fairly rare occasions when the critical slopes are being examined, the complex solution to the problem is not included and the interested reader may refer to "Rock Slope Engineering", by Hoek and Bray, 1981, or other relevant books.

*Definition of Wedge Geometry*

The geometry of the wedge, for the purpose of analyzing the basic mechanics of sliding, is defined in Figure 13.23. Note that, throughout this section, the flatter of the two planes is called Plane A while the steeper plane is called Plane B.

As in the case of plane failure, a condition of sliding is defined by $\psi_{fi} > \psi_i > \phi$, where $\psi_{fi}$ is the inclination of the slope face, measured in the view at right angles to the line of intersection, and $\psi_i$ is the dip of the line of intersection. Note that $\psi_{fi}$ would only be the same as the true dip of the slope face if the dip direction of the line of intersection was the same as the dip direction of the slope face.

*Analysis of Wedge Failure*

The factor of safety of the wedge defined in Figure 13.23b and c assuming that sliding is resisted by friction only and that the friction angle $\phi$ is the same for both planes, is given by:

$$F = \frac{(R_A + R_B)\ \tan\phi}{W.\sin\psi_i} \qquad (13.26)$$

where,

RA and RB are the normal reactions provided by planes A and B as illustrated in the sketch below.

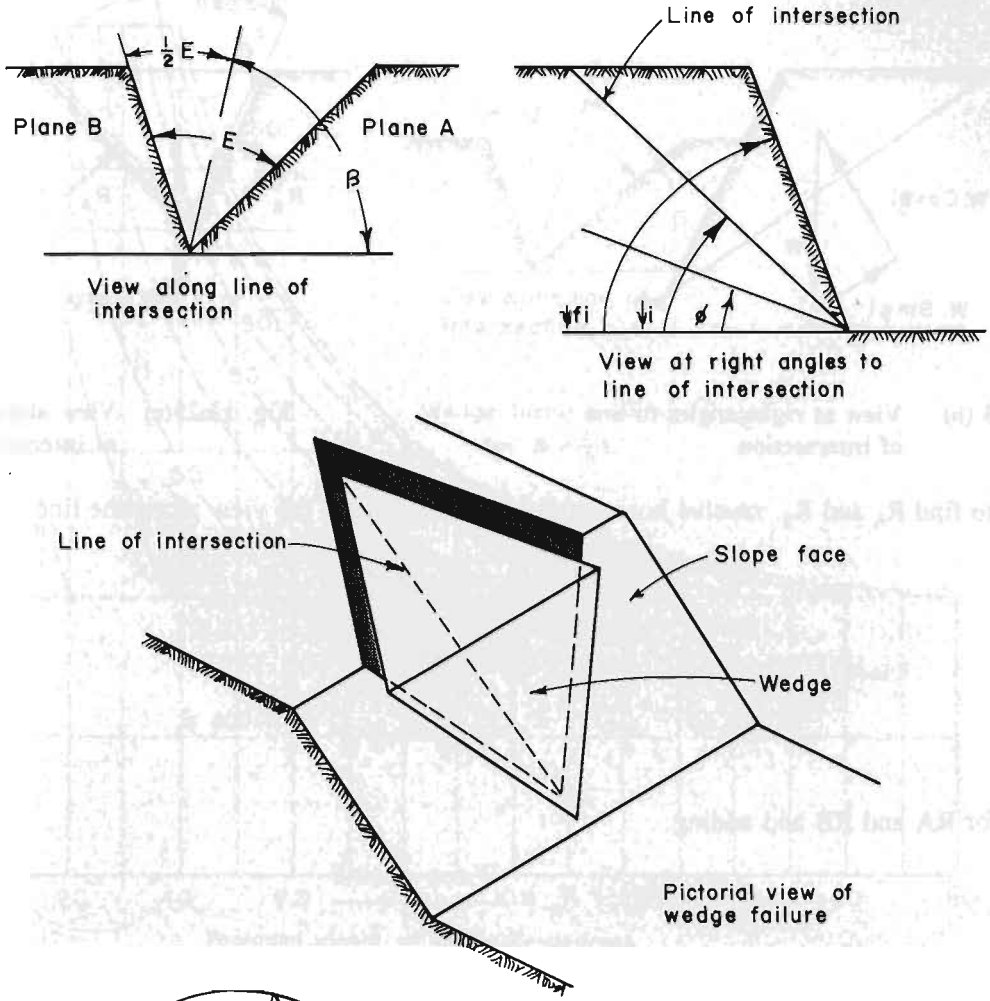


Source: USDT 1981

**Fig. 13.23a Wedge failure geometry**

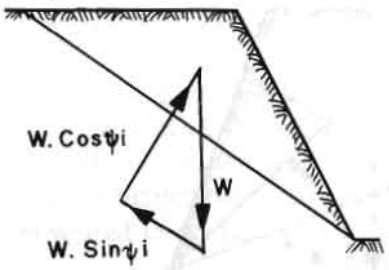


Fig. 13.23 (b) View at right angles to line of intersection

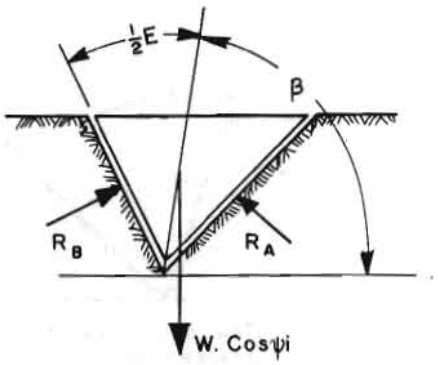


Fig. 13.23(c) View along line of intersection

In order to find $R_A$ and $R_B$, resolve horizontally and vertically in the view along the line of intersection:

$$R_A.\sin\ (\beta-\frac{1}{2}\xi)\ =\ R_B.\sin\ (B\ +\ \frac{1}{2}\xi) \tag{13.27}$$

$$R_A.\cos\ (\beta\ -\ \frac{1}{2}\xi)\ -\ R_B.\cos\ (\beta\ +\ \frac{1}{2}\ \xi)\ =\ W.\cos\ \psi_i\ . \tag{13.28}$$

Solving for RA and RB and adding:

$$R_A\ +\ R_B\ =\ \frac{W.\cos\ \psi_i.\sin\beta}{\sin\ \frac{1}{2}\ \xi}\ . \tag{13.29}$$

Hence,

$$F\ =\ \frac{\sin\beta}{\sin\frac{1}{2}\xi}\ .\ \frac{\tan\ \phi}{\tan\ \psi_i}\ . \tag{13.30}$$

In other words:

$$F_W\ =\ K.\ F_P \tag{13.31}$$

Where $F_W$ is the factor of safety of a wedge supported by friction only, $F_P$ is the factor of safety of plane failure in which the slope face is inclined at $\psi_{fi}$ and the failure plane is inclined at $\psi_i$.

K is the wedge factor which, as shown by Equation 13.30 depends upon the included angle of the wedge and upon the angle of tilt of the wedge. Values for the wedge factor, K, for a range of values of ß and $\xi$, are plotted in Figure 13.24.

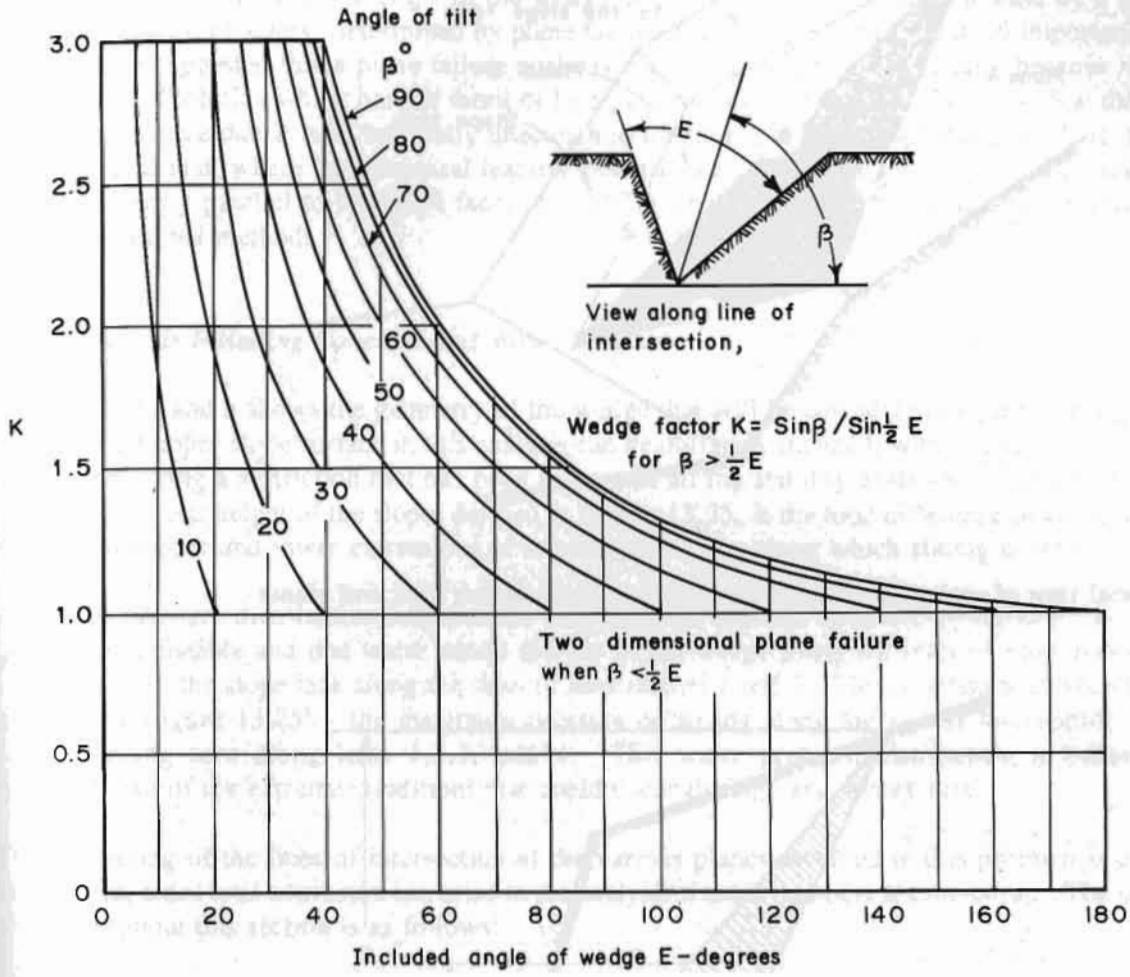


Source: USDT 1981

**Fig. 13.24 Wedge factor K as a function of wedge geometry**

As shown in the stereoplot given in Figure 13.23a, measurement of the angles ß and ξ can be carried out on the great circle, the pole of which is the point representing the line of intersection of the two planes. Hence, a stereoplot of the features that define the slope and the wedge geometry can provide all the information required for the determination of the factor of safety. It should, however, be remembered that the case that has been dealt with is very simple and that, when different friction angles and the influence of cohesion and water pressure are allowed for, the equations become more complex. Rather than develop these equations in terms of the angles ß and ξ, which cannot be measured directly in the field, the more complete analysis is presented in terms of directly measurable dips and dip directions.

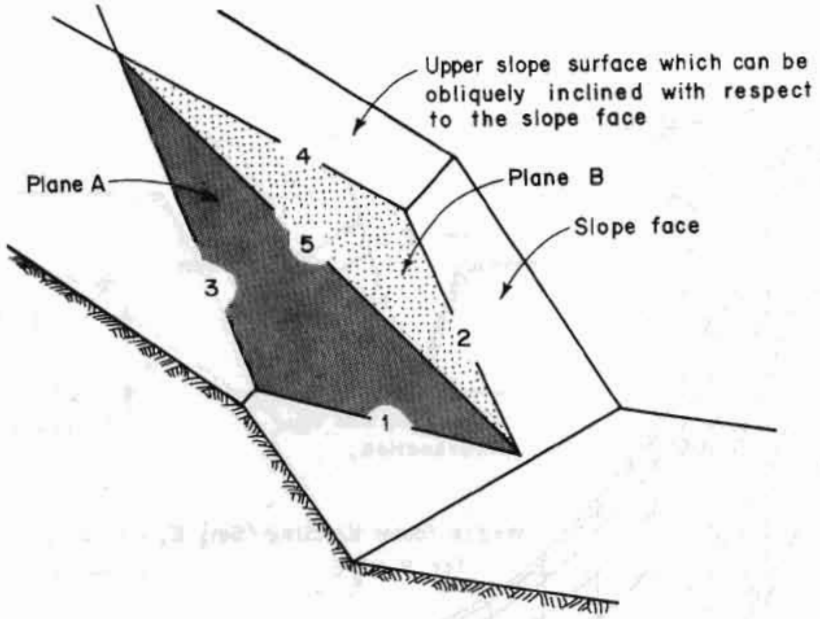


a) Pictorial view of wedge showing the numbering of intersection lines and planes

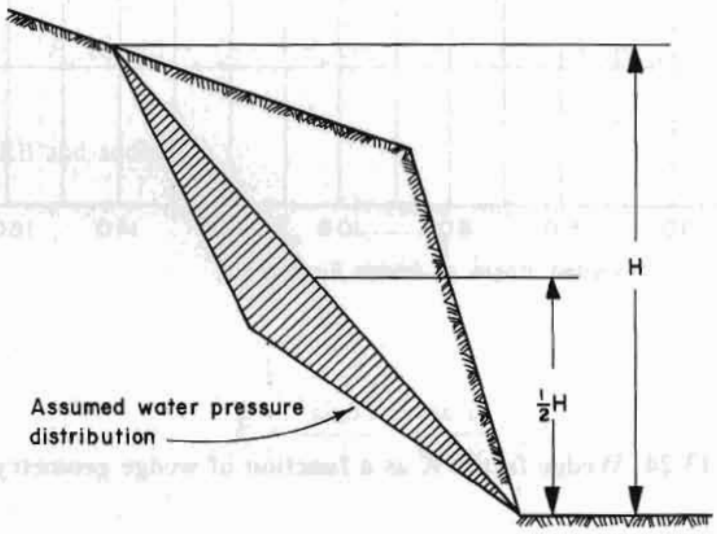


b) View normal to the line of intersection 5 showing the total wedge height and the water pressure distribution

Source: USDT 1981

**Fig. 13.25** Geometry of wedge used for stability analysis including the influence of cohesion and of water pressure on the failure surfaces

Before leaving this simple analysis, the reader's attention is drawn to the important influence of the wedging action as the included angle of the wedge decreases below 90°. The increase by a factor of 2 or 3 on the factor of safety, determined by plane failure analysis, is of great practical importance. Some experts have suggested that a plane failure analysis is acceptable for all rock slopes because it provides a lower bound solution which has the merit of being conservative. Figure 13.24 shows that this solution is so conservative that it is to be totally uneconomic for most practical slope designs. It is, therefore, recommended that, where the structural features that are likely to control the stability of a rock slope do not strike nearly parallel to the slope face, the stability analysis should be carried out by means of the three-dimensional method.

*Wedge Analysis Including Cohesion and Water Pressure*

Figure 13.25a and b shows the geometry of the wedge that will be considered in the following analysis. Note that the upper slope surface in this analysis can be obliquely inclined, with respect to the slope face, thereby removing a restriction that has been present in all the stability analyses discussed so far in this section. The total height of the slope, defined in Figure 13.25, is the total difference in vertical elevation between the upper and lower extremities of line of intersection along which sliding is assumed to occur.

The water pressure distribution, assumed for this analysis, is based upon the hypothesis that the wedge itself is impermeable and that water enters the top of the wedge along the lines of Intersection 3 and 4 and leaks from the slope face along the lines of Intersection 1 and 2. The resulting pressure distribution is shown in Figure 13.25b - the maximum pressure occurring along the line of Intersection 5 and the pressure being zero along lines 1,2,3, and 4. This water pressure distribution is believed to be representative of the extreme conditions that could occur during very heavy rain.

The numbering of the lines of intersection of the various planes involved in this problem is of extreme importance, since total confusion can arise in the analysis if these numbers are mixed-up. The numbering used throughout this section is as follows:

1 - intersection of plane A with the slope face,
2 - intersection of plane B with the slope face,
3 - intersection of plane A with the upper slope surface,
4 - intersection of plane B with the upper slope surface, and
5 - intersection of planes A and B.

It is assumed that sliding of the wedge always takes place along the line of the intersection numbered 5.

The factor of safety of this slope is derived from the detailed analysis of this problem published by Hoek and Bray (1981).

$$F = \frac{3}{\gamma H}\,(c_A.X + c_B.\gamma) + (A - \frac{\gamma_w}{2\gamma}.X)\,\tan\phi_A + (B - \frac{\gamma_w}{2\gamma}.Y)\,\tan\phi_B \qquad (13.32)$$

where,

$c_A$ and $c_B$ are the cohesive strengths of planes A and B,
$\phi_A$ and $\phi_B$ are the angles of friction on planes A and B,
$\gamma$ is the unit weight of the rock,
$\gamma_w$ is the unit weight of water, and
H is the total height of the wedge (Fig. 13.25b).

X,Y,A, and B are dimensionless factors that depend upon the geometry of the wedge.

$$X = \frac{\sin\theta_{24}}{\sin\theta_{45}.\cos\theta_{2na}} \tag{13.33}$$

$$Y = \frac{\sin\theta_{13}}{\sin\theta_{35}.\cos\theta_{1nb}} \tag{13.34}$$

$$A = \frac{\cos\psi_a - \cos\psi_b.\cos\theta_{na.nb}}{\sin\psi_5.\sin^2\theta_{na.nb}} \tag{13.35}$$

$$B = \frac{\cos\psi_b - \cos\psi_a.\cos\theta_{na.nb}}{\sin\psi_5.\sin^2\theta_{na.nb}} \tag{13.36}$$

where $\psi_a$ and $\psi_b$ are the dips of planes A and B respectively and $\psi_5$ is the dip of the line of Intersection 5.

The angles required for the solution of these equations can most conveniently be measured on a stereoplot of the data that defines the geometry of the wedge and the slope.

Consider the following example:

| Plane | Dip° | Dip direction° | Properties |
|---|---|---|---|
| A | 45 | 105 | $\phi_A = 20_o$, $C_A = 500$ lb/ft$^2$ |
| B | 70 | 235 | $\phi_B = 30_o$, $C_B = 1000$ lb/ft$^2$ |
| Slope face | 65 | 185 | $\gamma = 160$ lb/ft$^3$ |
| Upper surface | 12 | 195 | $\gamma_w = 62.5$ lb/ft$^3$ |

The total height of the wedge H = 130 ft.

The stereoplot of the great circles representing the four planes, involved in this problem, is presented in Figure 13.26 and all the angles required for the solution of Equations 13.33 to 13.36 are marked in this figure.

Determination of the factor of safety is most conveniently carried out on a calculation sheet such as that presented in Table 13.2. Setting the calculations out in this manner not only enables the user to check all the data but it also shows how each variable contributes to the overall factor of safety. Hence, if it is necessary to check the influence of the cohesion on both planes falling to zero, this can be done by setting the two groups containing the cohesion values $c_A$ and $c_B$ to zero, giving a factor of safety of 0.62. Alternatively, the effect of drainage can be checked by putting the two water pressure terms (i.e., those containing $\gamma_w$) to zero, giving F = 1.98. As has been emphasized in previous sections, this ability to check the sensitivity of the factor of safety to changes in material properties or in slope loading is probably as important as the ability to calculate the factor of safety itself.

*Wedge Stability Charts for Friction Only*

If the cohesive strength of the planes A and B is zero and the slope is fully drained, Equation 13.32 reduces to:

$$F = A.\tan \phi_A + B.\tan \phi_B \quad . \tag{13.37}$$

The dimensionless factors A and B are found to depend upon the dips and dip directions of the two planes; values of these two factors have been computed for a range of wedge geometries and the results are presented as a series of charts on the following pages (Fig. 13.27).

In order to illustrate the use of these charts, consider the following example:

| | Dip° | Dip Direction° | Friction Angle° |
|---|---|---|---|
| Plane A | 40 | 165 | 35 |
| Plane B | 70 | 285 | 20 |
| | --- | --- | |
| Differences | 30 | 120 | |

Hence, turning to the charts headed "Dip difference 30°", and reading off the values of A and B for a difference in dip direction of 120°, one finds that A = 1.5 and B = 0.7.

Substitution in Equation 13.37 gives the factor of safety as F = 1.30. The values of A and B give a direct indication of the contribution that each of the planes makes to the total factor of safety.

Note that the factor of safety calculated from Equation 13.37 is independent of the slope height, the angle of the slope face, and the inclination of the upper slope surface. This rather surprising result arises because the weight of the wedge occurs in both the numerator and denominator of the factor of safety equation and for the friction only case. This term cancels out, leaving a dimesionless ratio that defines the factor of safety (see Equation 13.30).

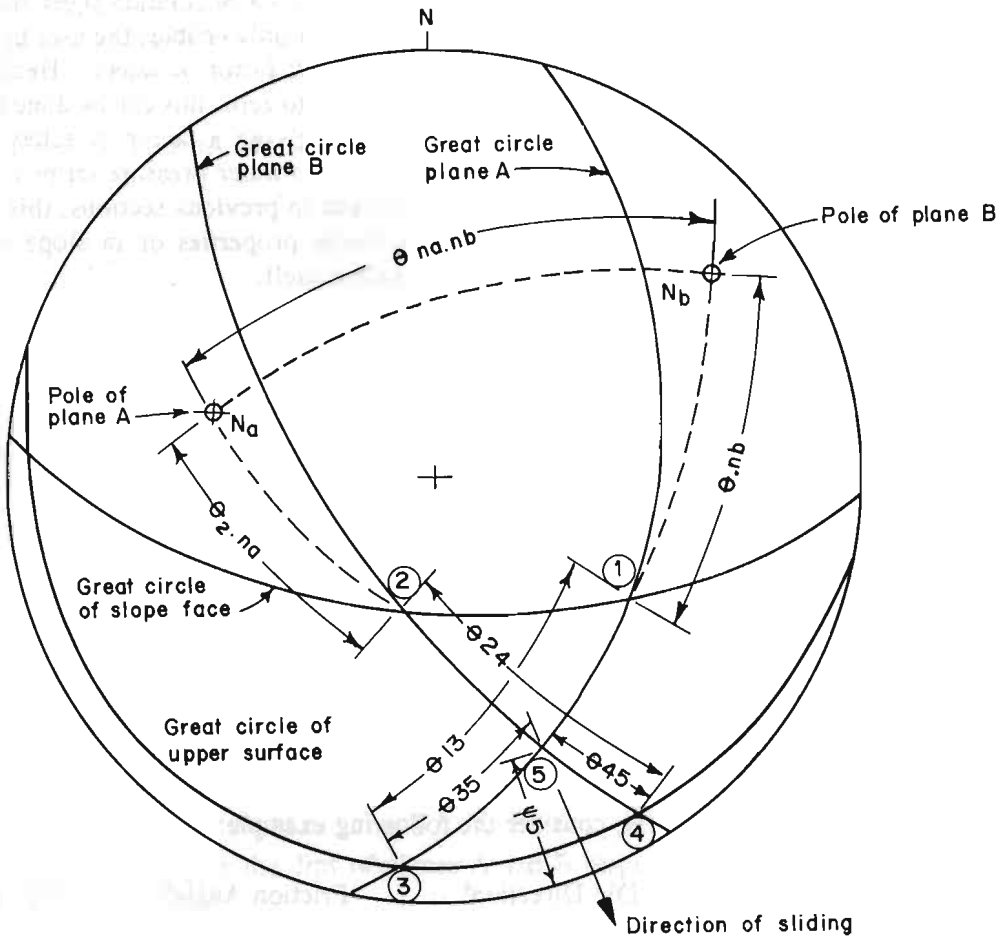


Source: USDT 1981

**Fig. 13.26 Stereoplot of data required for wedge stability analysis**

This simplification is very useful in that it enables the user of these charts to carry out a very quick check on the stability of a slope on the basis of the dips and dip directions of the discontinuities in the rock mass into which the slope has been cut. An example of such an analysis is presented later in this chapter.

Many trial calculations have shown that a wedge, having a factor of safety in excess of 2.0, as obtained from the friction only stability charts, is unlikely to fail under even the most severe combination of conditions to which the slope is likely to be subjected. Consider the example discussed earlier in which the factor of safety for the worst conditions (zero cohesion and maximum water pressure) is 0.62.

## WEDGE STABILITY CALCULATION SHEET

| INPUT DATA | FUNCTION VALUE | CALCULATED ANSWER |
|---|---|---|
| $\psi_a = 45°$<br>$\psi_b = 70°$<br>$\psi_5 = 31.2°$<br>$\theta_{na.nb} = 101°$ | $\cos\psi_a = 0.7071$<br>$\cos\psi_b = 0.3420$<br>$\sin\psi_5 = 0.5180$<br>$\cos\theta_{na.nb} = -0.191$<br>$\sin\theta_{na.nb} = 0.982$ | $A = \dfrac{\cos\psi_a - \cos\psi_b.\cos\theta_{na.nb}}{\sin\psi_5.\sin^2\theta_{na.nb}} = \dfrac{0.7071 + 0.342 \times 0.191}{0.5180 \times 0.9636} = 1.5475$<br>$B = \dfrac{\cos\psi_b - \cos\psi_a.\cos\theta_{na.nb}}{\sin\psi_5.\sin^2\theta_{na.nb}} = \dfrac{0.3420 + 0.7071 \times 0.191}{0.5180 \times 0.9636} = 0.9557$ |
| $\theta_{24} = 65°$<br>$\theta_{45} = 25°$<br>$\theta_{2.na} = 50°$ | $\sin\theta_{24} = 0.9063$<br>$\sin\theta_{45} = 0.4226$<br>$\cos\theta_{2.na} = 0.6428$ | $X = \dfrac{\sin\theta_{24}}{\sin\theta_{45}.\cos\theta_{2.na}} = \dfrac{0.9063}{0.4226 \times 0.6428} = 3.3363$ |
| $\theta_{13} = 62°$<br>$\theta_{35} = 31°$<br>$\theta_{1.nb} = 60°$ | $\sin\theta_{13} = 0.8829$<br>$\sin\theta_{35} = 0.5150$<br>$\cos\theta_{1.nb} = 0.5000$ | $Y = \dfrac{\sin\theta_{13}}{\sin\theta_{35}.\cos\theta_{1.nb}} = \dfrac{0.8829}{0.5150 \times 0.500} = 3.4287$ |
| $\phi_A = 30°$<br>$\phi_B = 20°$<br>$\gamma = 160\ lb/ft^3$<br>$\gamma_w = 62.5\ lb/ft^3$<br>$c_A = 500\ lb/ft^2$<br>$c_B = 1000\ lb/ft^2$<br>$H = 130\ ft$ | $\tan\phi_A = 0.5773$<br>$\tan\phi_B = 0.3640$<br>$\gamma_w/2\gamma = 0.1953$<br>$3c_A/\gamma H = 0.0721$<br>$3c_B/\gamma H = 0.1442$ | $F = \dfrac{3c_A}{\gamma H}.X + \dfrac{3c_B}{\gamma H}.Y + \left(A - \dfrac{\gamma_w}{2\gamma}.X\right)\tan\phi_A + \left(B - \dfrac{\gamma_w}{2\gamma}.Y\right)\tan\phi_B$<br>$F = 0.2405 + 0.4944 + 0.8934 - 0.3762 + 0.3478 - 0.2437 = 1.3562$ |

Table 13.2 Wedge Stability Table

This is 50 per cent of the factor of safety of 1.24 for the friction only case. Hence, had the factor of safety for the friction only case been 2.0, the factor of safety for the worst conditions would have been 1.0, assuming that the ratio of the factors of safety for the two cases remains constant.

On the basis of such trial calculations, Hoek and Bray (1981) suggested that the friction only stability charts can be used to define those slopes that are adequately stable and that can be ignored in subsequent analyses. Such slopes, having a factor of safety in excess of 2.0, pass into the stable category. Slopes with a factor of safety, based upon friction only, of less than 2.0 must be regarded as being in the potentially unstable category, i.e., these slopes require further detailed examination. In many cases, there are a number of wedges that may slide in chain reaction, one after another, as support provided by adjoining wedges is lost. This possibility should be studied in detail (Wagner et al. 1988).

In many practical problems involving the design of the cut slopes for a highway, it will be found that these friction only stability charts provide all the information that is required. It is frequently possible, having identified a potentially dangerous slope, to eliminate the problem by a slight realignment of the benches or of the road alignment. Such a solution is clearly only feasible if the potential danger is recognized before excavation of the slope is started, and the main use of the charts is during the site investigation and preliminary planning stage of a slope project.

Once a slope has been excavated, these charts will be of limited use since it will be fairly obvious if the slope is unstable. Under these conditions, a more detailed study of the slope will be required and use would then have to be made of the analytical solution. In Hoek and Bray's experience (1981) relatively few slopes require this detailed analysis and the reader should beware of wasting time on such an analysis when the simpler methods presented in this chapter would be adequate. A full stability analysis may look very impressive in a report but, unless it has enabled the slope engineer to take positive remedial measures, it may have served no useful purpose.

Computer Programmes SASP and SASW for wedge failure are available for rapid computation of static and dynamic factors of safety for any number of joint sets. The programmes also account for submergence of rock slopes. Programme SASP gives cut slope angle for a given factor of safety. For rigorous analysis of wedges with tension cracks, inclined top terraces, and rock bolts, the programme known as WEDGE may be used.

## 13.5 LANDSLIDES

Any attempt to predict landslides and to stabilize existing landslides requires a thorough understanding of the causes of landslides and the mechanics of stability. The discussions in the preceding chapters help to understand the mechanics of stability.

It may be recalled that almost all slope failures primarily fall into one of the three categories: planar, rotational, and toppling. However, a large landslide may contain several types of failure through its width, height, and depth due to the heterogeneity and anisotropy of the material. Once a large landslide has occurred and the landslide mass is momentarily remaining stable, it is vulnerable to smaller slides within the mass and to reactivation of the entire slide mass, depending upon the extent of causative factors over time. Landslides are, in many instances, themselves the cause of new landslides in adjoining areas which were otherwise stable. This is so because the adjoining areas are then exposed and subject to surface erosion, gullying, toe erosion, weathering, and freedom of movement.

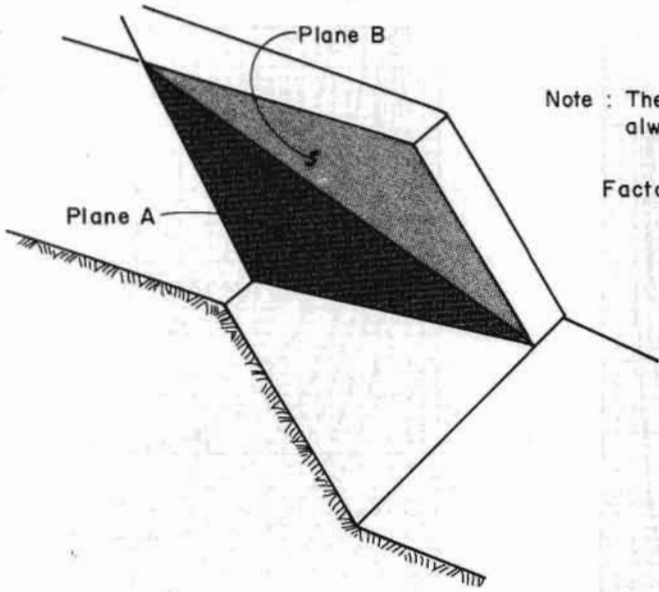


Note : The flatter of the two planes is always called plane A.

Factor of safety

$$F = A.\,Tan\phi_A + B.\,Tan\phi_B$$

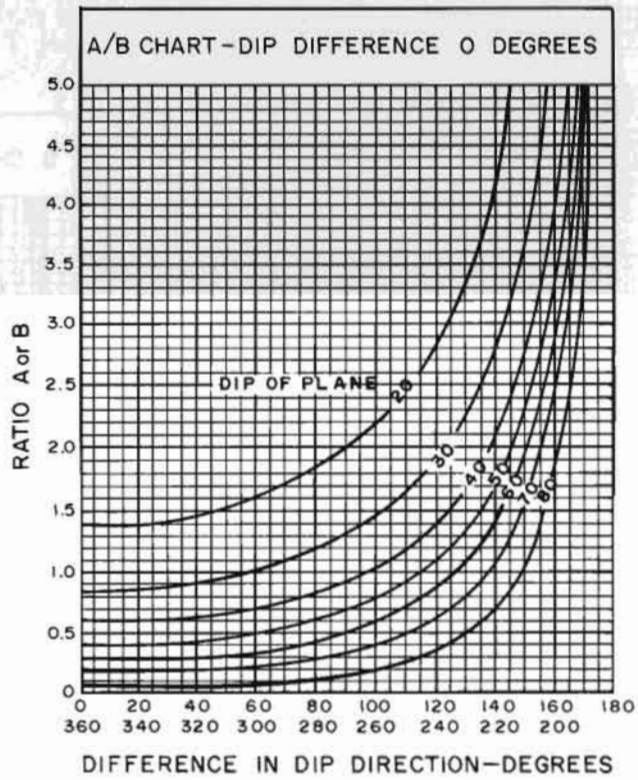


Source: USDT 1981

**Fig. 13.27 Wedge stability charts for friction only**

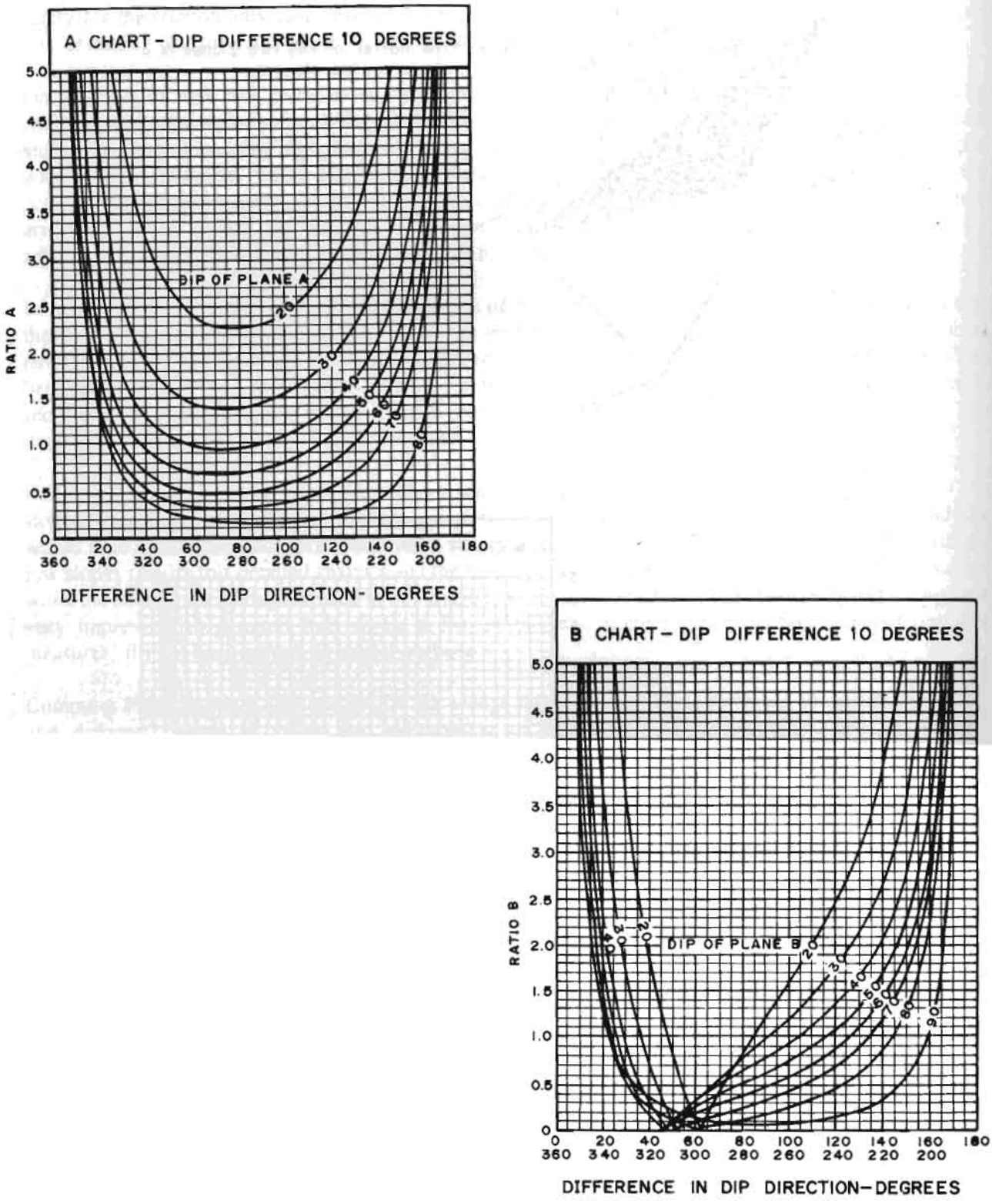


Fig. 13.27 Wedge stability charts for friction only (contd.)

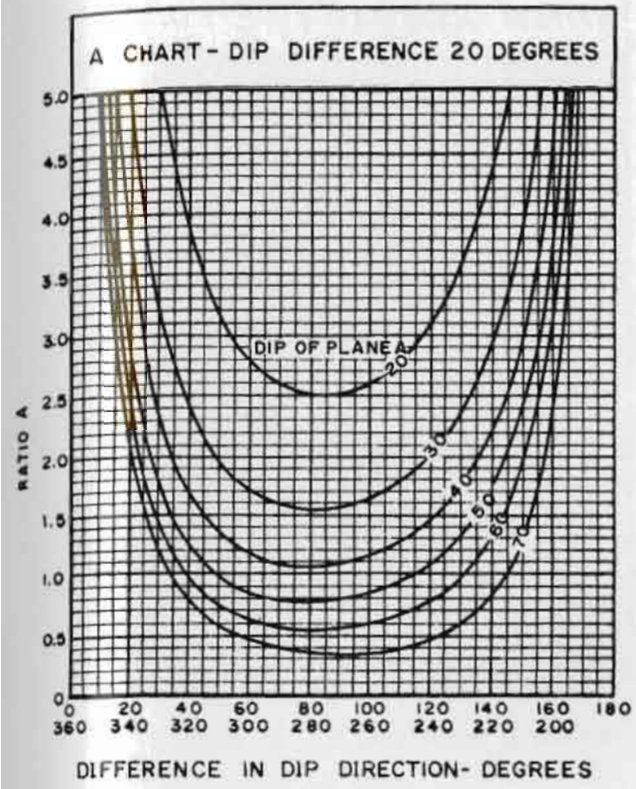


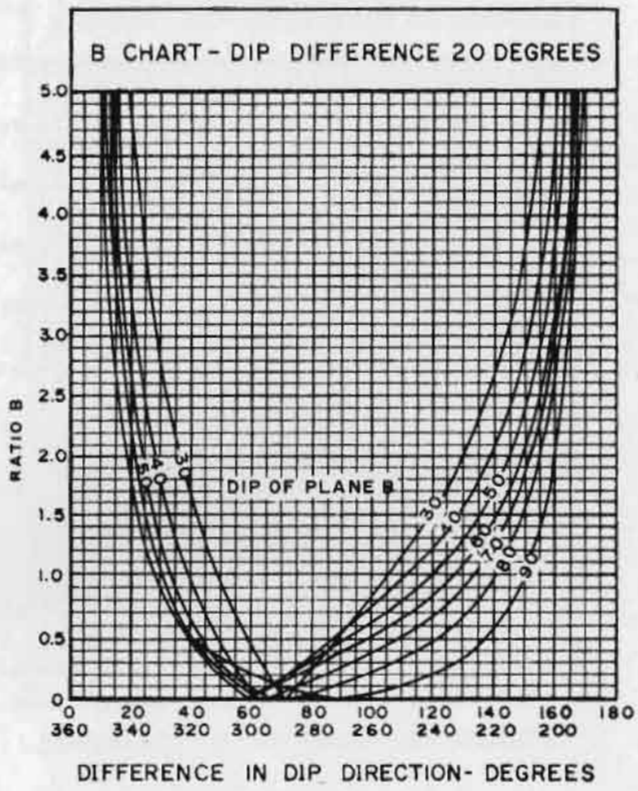


**Fig. 13.27 Wedge stability charts for friction only (contd.)**

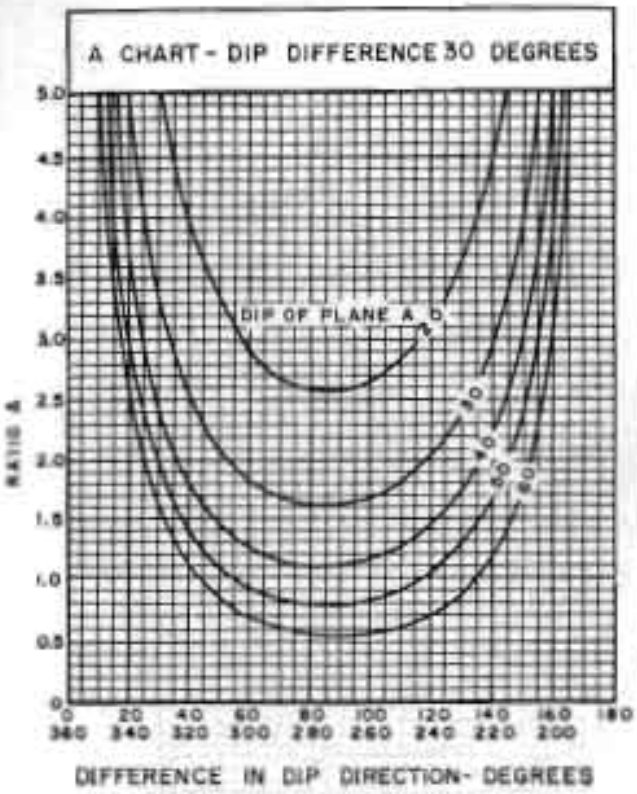


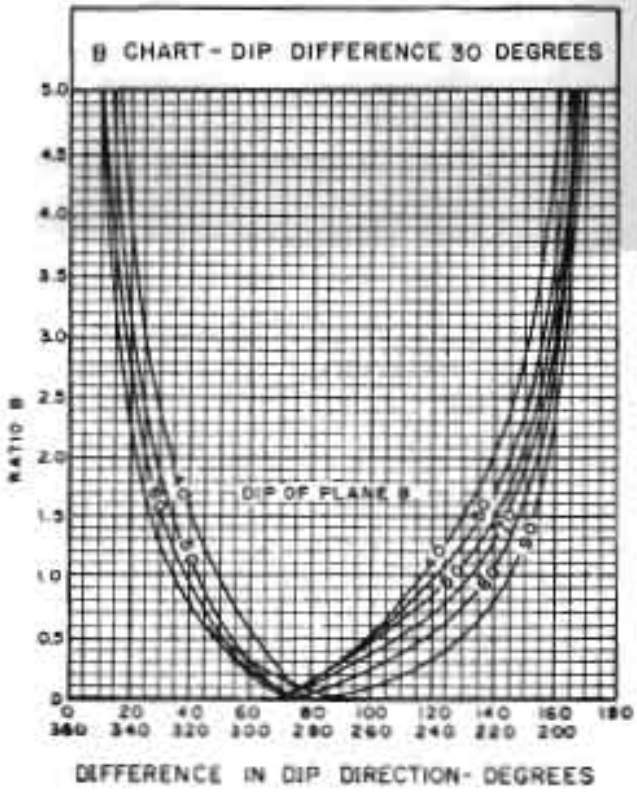


Fig. 13.27 Wedge stability charts for friction only (contd.)

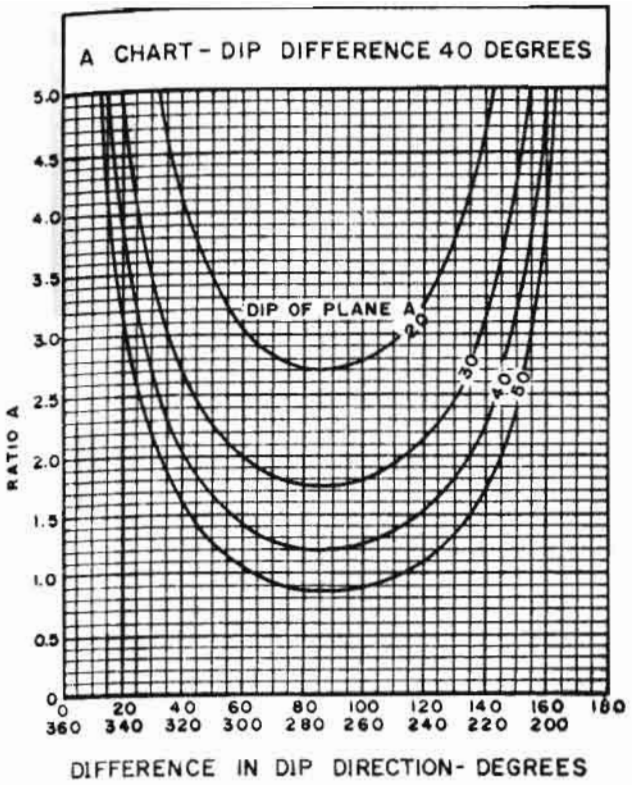


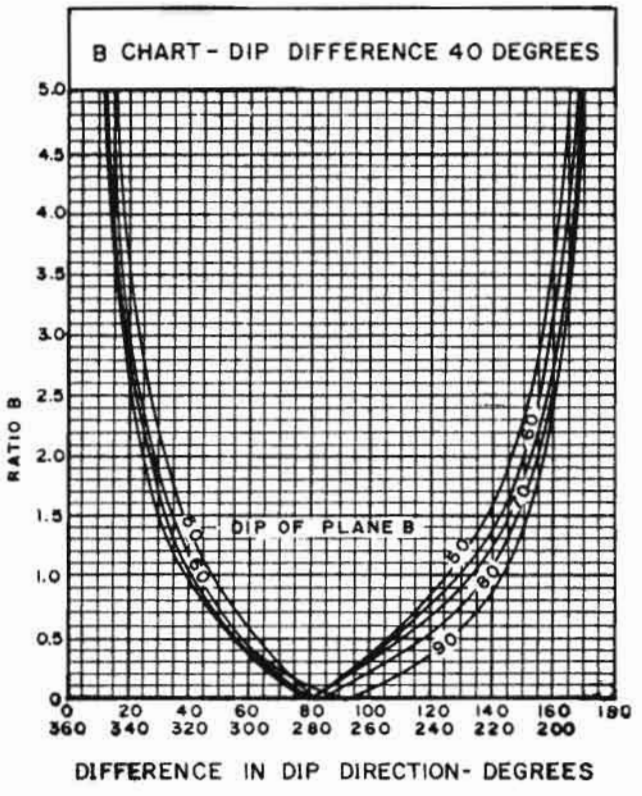


**Fig. 13.27 Wedge stability charts for friction only (contd.)**

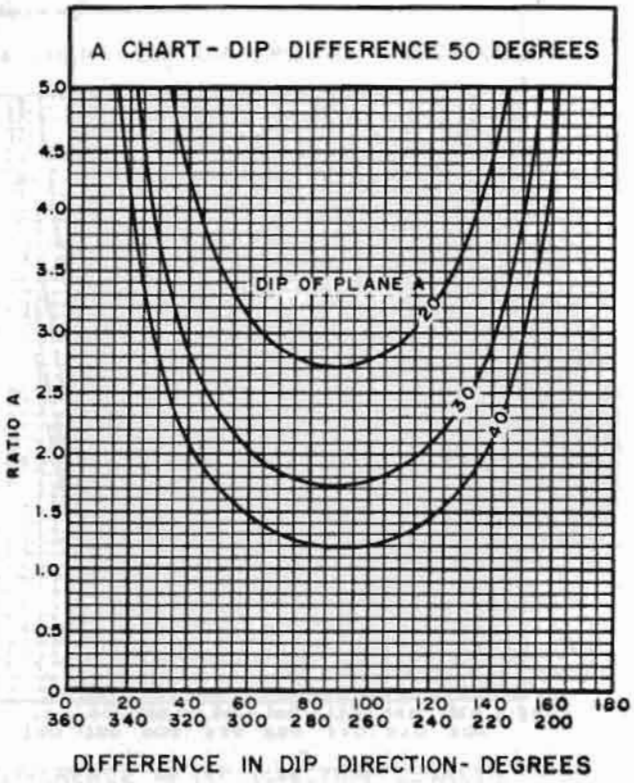


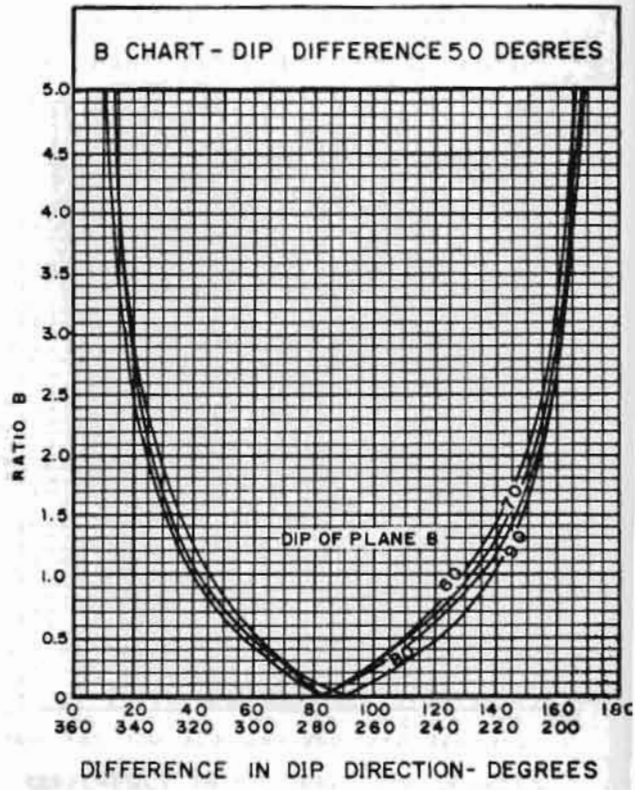


Fig. 13.27 Wedge stability charts for friction only (contd.)

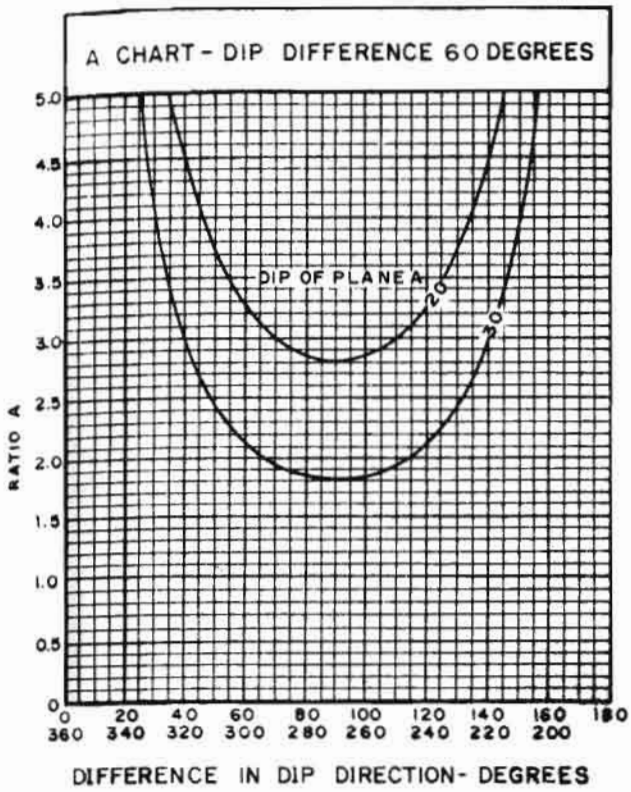


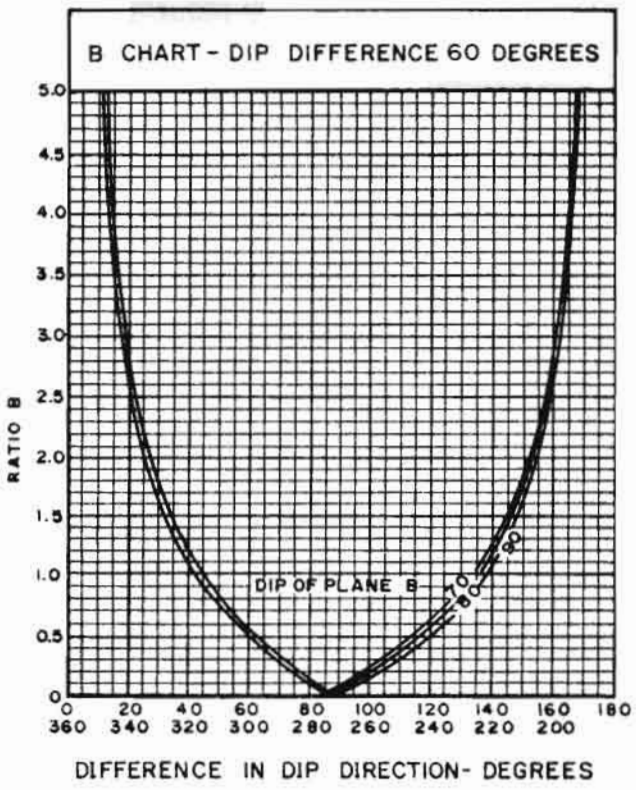


Fig. 13.27 Wedge stability charts for friction only (contd.)

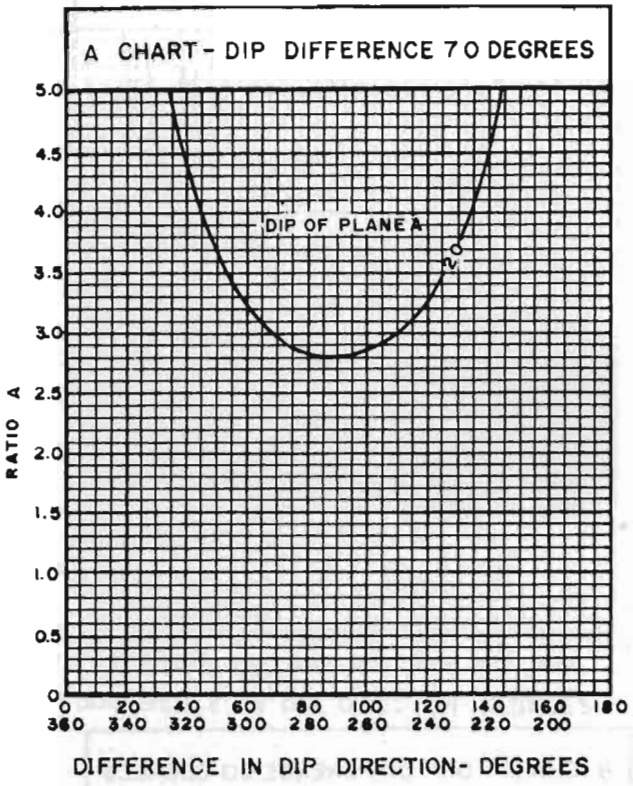


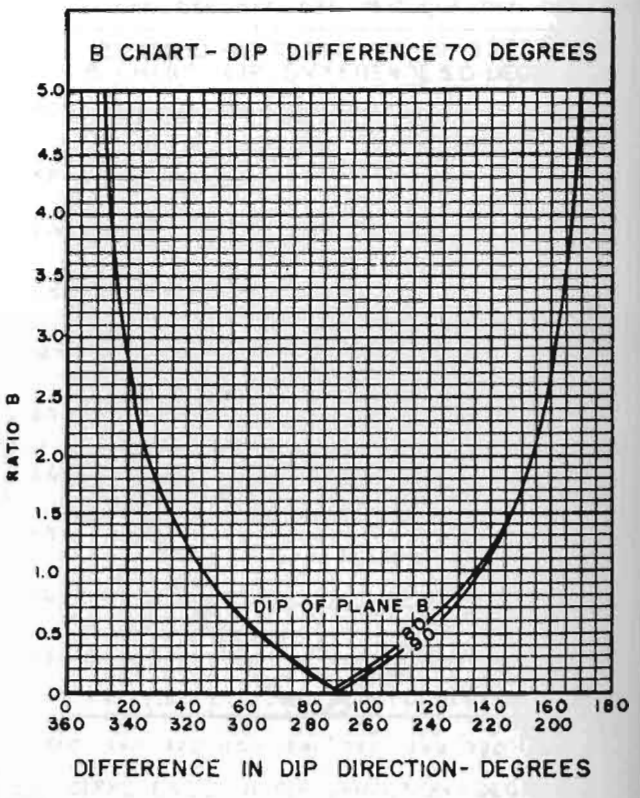


**Fig. 13.27 Wedge stability charts for friction only (contd.)**

The following discussion is aimed at an understanding of landslides in order to plan and design appropriate stabilization measures.

### 13.5.1 *Causes of Landslides*

The major causes of landslides are not the same as the causes of triggering of slides. It is useful to understand both of them.

*Landslide Trigger*

(i) Cloud burst (200-1000 mm per day)
(ii) Uncontrolled flow of water on slope surface from overflooded steep gullies.
(iii) Toe cutting may activate failure by overtoppling of rock blocks or slides in colluvium.
(iv) Earthquake vibrations.
(v) Blasting vibrations.
(vi) Flash flood due to glacier lake outburst/failure of landslide dam/cloudburst, etc.

*Major Causes of Landslide*

Man-made causes

(i) Large-scale indiscriminate deforestation.
(ii) Large-scale indiscriminate blasting and quarrying.
(iii) Excessive hill cutting, daylighting planes of weakness followed by toe erosion.
(iv) Intense agricultural operations, such as irrigation of paddy fields and water storage ponds, above the hill slope.
(v) Mass-scale construction of houses, sewerage systems, and heavy structures on the entire hill.
(vi) Submergence by lakes, dam reservoirs, and canals
(vii) Side-casting or throwing excavated material downhill (throwing of landslide material on to the road triggers the slide again because of loss of toe support).
(viii) Vibrations of heavy vehicles on the hill road.
(ix) Undermining caused by mining and tunnelling.

Erosion Process

(x) Blocking of natural drainage systems and narrow culverts by logs, boulders, and gully bank slides.

(xi) High flow velocities in steep gullies move very large boulders that will destroy roads, culverts, and the ecosystem.

(xii) Large-scale slide of banks along steep gullies or *nalas* can even block the river after very long spells of continuous rain and form a landslide-dam.

(xiii) Uncontrolled flow of rainwater on slope surface washes out soil and boulders.

(xiv) Wind erosion leads to the formation of heaps of loose soil or slope material (thin chips of rocks) on the road; it is not, however, a major problem in the Himalayan Region.

Pore-water Pressure due to Adverse Hydrogeological Conditions

(xv) Groundwater table rises up temporarily in the monsoon. It washes out the cementing material from soil and rock masses.

(xvi) Perched water table builds up very fast in the monsoon on impervious surfaces, e.g., clay seams, clay layers, bedrocks, etc.

(xvii) Water pressure in tension cracks not only pushes the slope forward but it also generates pore-water pressure along joints or bedding planes. As the slide starts, the opening of the rough joints increases due to dilatation. Thus the plane of sliding acts as a natural channel for the flow of water.

(xviii) Seepage from choked catch drains may raise pore-water pressure along the slip surface.

(xix) Inadequate size and choking of roadside drains may also lead to the same problem.

(xx) Pressure of aquifers, such as sand layers or sandstone layers (in between impervious beds) can cause very high pore-water pressure on overlying layers in slopes in sedimentary deposits.

(xxi) Saturation destroys capillary tension in soils and reduces its cohesion because of the increase in moisture content. Earthquake may liquefy loose, fine soil and seams in the rock mass.

Adverse Geological Conditions

(xxii) Dips of bedding planes, clay seams, or weak rock layers are nearly the same as those of the slope causing planar sliding. (Thin beds may buckle due to self-weight on very high slopes.)

(xxiii) Dip direction of joint set is nearly the same as that of the slope ($\pm$ 20°).

(xxiv) Greater number of unfavourably-oriented joint sets with many wedges.

(xxv) Weathering of rock mass.

(xxvi) Slope material is loose, cohesionless material, e.g., colluvium, soil, etc.

(xxvii) Huge boulders are sitting on the hill surface and are likely to topple or slide down.

(xxviii) Steeply dipping joints or bedding planes may lead to slope failure by overtoppling of rock blocks.

(xxix) Talus or debris contains fines and clay friction.

(xxx) Clay seams, etc. have low coefficient of friction and so sliding takes place easily.

(xxxi) Pre-existing slip surface in old landslide areas can be reactivated because of adverse hydrogeological conditions.

(xxxii) Swelling clay/sensitive clay/fissured over consolidated clay is present and loses strength because of water absorption/disturbance/release of stress during cutting.

(xxxiii) Soluble rocks with solution cavities.

(xxxiii) High tectonic stress will lead to heaving and buckling of layers at the bottom of the pit after removal of the overburden. High tectonic stresses will also result in excessive deformation on the cut slope until locked-up strain energy is released.

*Progressive Failure*

Theoretically cut slopes should fail in the first intense monsoon wherever conditions for sliding exist. However, in reality, slopes may fail progressively for several years. If corrective measures are not taken in time, failure may progress slowly upwards to several hundred metres. Eventually it may reach the top of the mountain.

Another interesting observation is that some rock slopes fail violently releasing a vast amount of stored strain energy in the form of rock blocks moving with great speed. However, such failures are rare. Violent failure is possible along pre-existing, non-circular surfaces of weakness only because movement is locked in until brittle failure of the hard rock occurs.

Intensive field research is needed in order to know more about landslides in the *Himalaya*. Natural landslides may be more difficult to understand and control. These are defined as landslides caused by natural causes. Man-made landslides are defined as those caused by man-made causes (as discussed above).

### 13.5.2 *Mechanics of Landslides*

Once the landslide has taken place, it is easier to know the mechanics of the landslide. It may be recalled that the mode of sliding may be idealized for simple and common landslides as given below.

*Rock Slope*

(i) Planar Sliding.
(ii) Wedge sliding along two joint planes.
(iii) Circular wedge sliding.
(iv) Dip sliding/sliding of regolith (Crozier 1986).

*Soil/Talus Slope*

(v) Talus or debris slide along bedrock/clay seam (just like dip sliding) in case of dip slopes in talus.
(vi) Circular wedge sliding in homogeneous soil mass or colluvium.

*Gullies*

(vii) Circular/plane wedge sliding along banks

(viii) Landslide debris flow like a viscous fluid (Sassa 1985) depending upon clay fraction, kinetic friction, etc.

*Rock Fall Jumping*

(ix) Smaller rock blocks will come down, bouncing along the rock slope or steep gully with rocky beds upto distances of serveral kilometres even if the slope is very gentle.

There are many landslides in which slope movement is frightening and complex, but the mechanics of the initial slide are simple as discussed above. For example, slope movement in the case of debris flow on dip slopes consists of a series of tension cracks, followed by slumps and slides, and finally appearing as a mudflow. It may be idealized as in the case of a high perched water table. Further complex rockfalls may be the result of dip sliding far above the road.

The real challenge is to analyse the huge complex landslides where different modes of failure are occurring at the top, middle, and bottom of the landslide. Each slide is unique and its corrective measures are also unique. In such difficult situations the advice of a team of experts and a geologist should be taken; for which detailed investigations would be necessary.

### 13.5.3 *Back Analysis of Landslides*

Before suggesting corrective measures, it would be better to back-analyse failed slopes to find out the shear strength parameters of the natural slope material. The method of back analysis is now easy using computer programmes.

i) The BASC Programme for the Back Analysis of (soil/rock) Slopes with Circular Wedge Failures (Singh and Ramasamy 1979).

ii) The BAST Programme for Back Analysis of Talus/Debris/Regolith/Dip Slope Failures.

iii) The BASP Programme for Back Analysis of Rock Slope with Plane Wedge Failure.

The shear strength parameters should then be used to study the stability of slopes with suitable corrective measures.

### 13.5.4 *Design Factors of Safety*

The design factors of safety for stable or stabilized slopes in the worst conditions should be as follows:

*Soil Slopes*

| | |
|---|---|
| Static factor of safety | 1.50 |
| Dynamic factor of safety | 1.0 |
| or | |
| Dynamic displacement | < 1 m or 1 per cent of slope height |

*Rock Slopes*

| | |
|---|---|
| Static factor of safety | 1.20 |
| Dynamic factor of safety | 1.0 |
| or | |
| Dynamic displacement | < 1 m or 1 per cent of slope height |